Laboratory of Computational Photochemistry and Photobiology
Dipartimento di Biotecnologia, Chimica e Farmacia - **Università di Siena**
Chemistry Department - **Bowling Green State University**

LCPP

On the Origin of the High Quantum Efficiency of Visual Pigments

Massimo Olivucci

VISTA, 22 June 2022

Department of Biotechnology, Chemistry and Pharmacy
Università di Siena

Emanuele Marsili

Laura Pedraza-González

MIUR

Fondazione
Banca d'Italia

Chemistry Department
Bowling Green State University

Xuchun Yang

Alejandro Blanco Gonzalez

Ohio Supercomputer Center
An OH·TECH Consortium Member

BGSU
Bowling Green State University

NATIONAL INSTITUTES OF HEALTH

NSF

Structure of Rhodopsins

hν
VIS (ca. 500 nm)

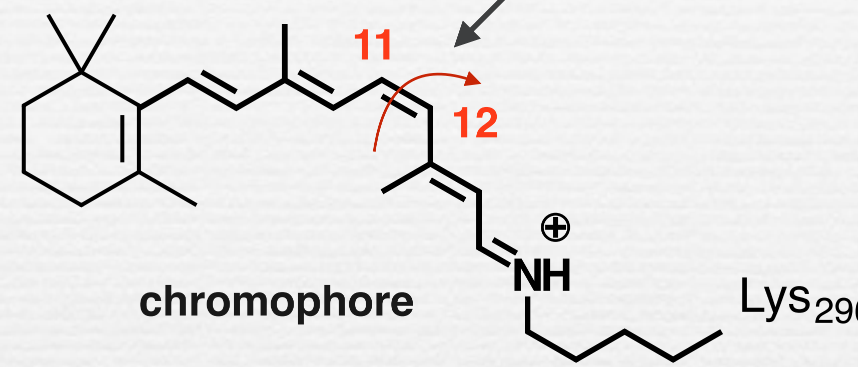

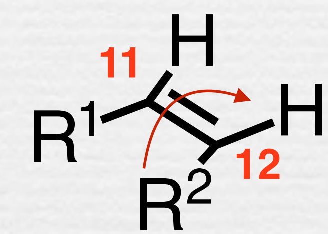

Obs. QY ca. 67%

chromophore or biomimetic molecular switch in solution:

Obs. QY ca. 20%

- Ernst, O. P.; Lodowski, D. T.; Elstner, M.; Hegemann, P.; Brown, L. S.; Kandori, H. *Chem. Rev.* **2014**, *114,* 126-63.
- Gozem, S.; Luk, H. L.; Schapiro, I.; Olivucci, M. *Chem. Rev.* **2017**, *117*, 13502-13565.

Electronic structure of the retinal chromophore

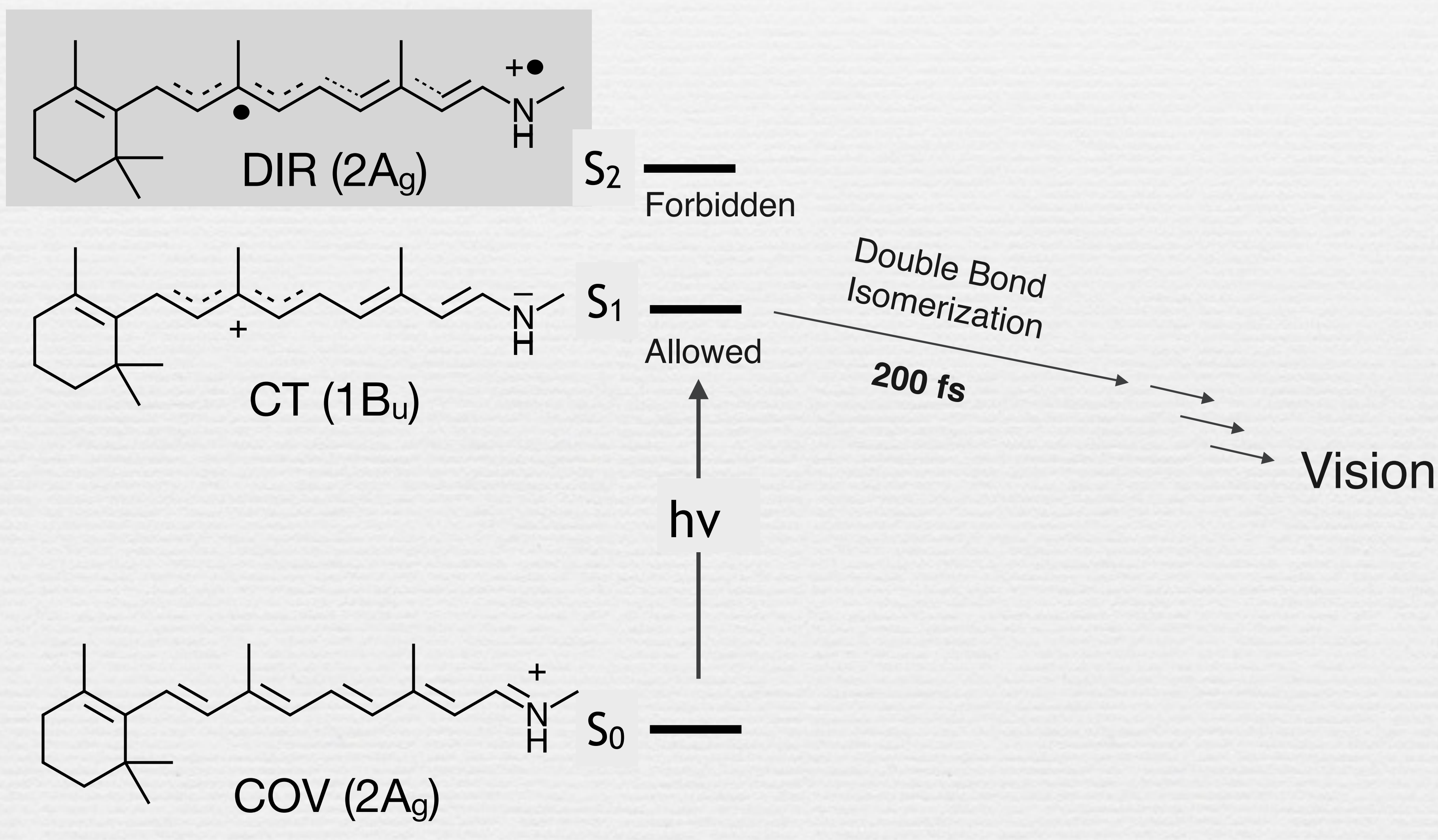

- Gozem, S.; Luk, H. L.; Schapiro, I.; Olivucci, M. *Chem. Rev.* **2017**, *117*, 13502-13565.

Mechanism of an ultrafast photochemical reaction

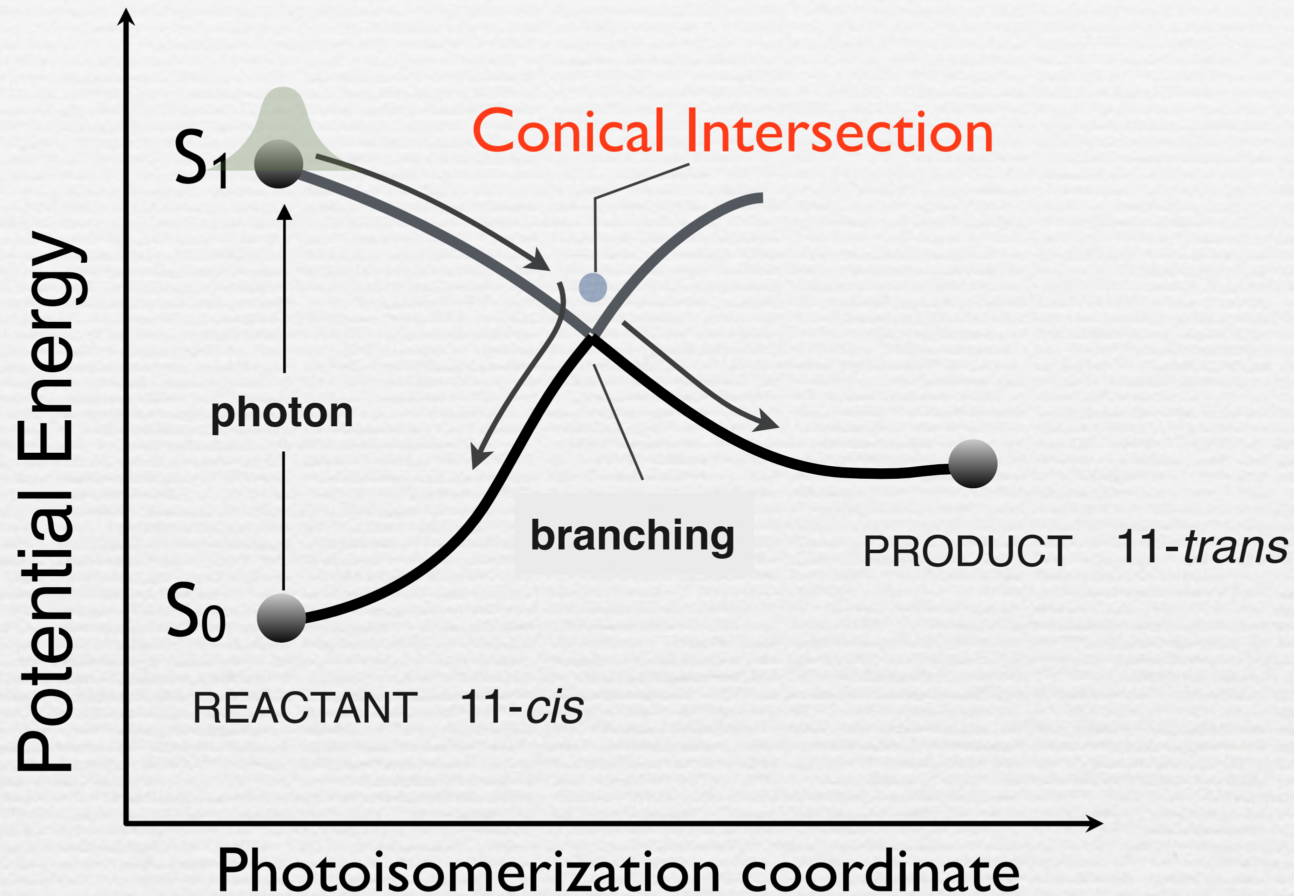

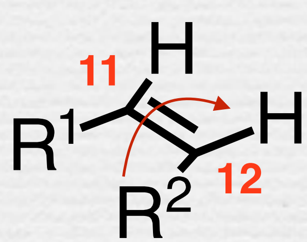

The Landau-Zener model is valid for a single-mode coordinate:

$$P = \exp\left(-\frac{2\pi H_{12}^2}{\hbar|vF|}\right)$$

probability of forming the product

velocity along the coordinate

difference in slopes of S_1 and S_0 along the coordinate

- Gozem, S.; Luk, H. L.; Schapiro, I.; Olivucci, M. *Chem. Rev.* **2017**, *117*, 13502-13565.

QM/MM models generated Automatically

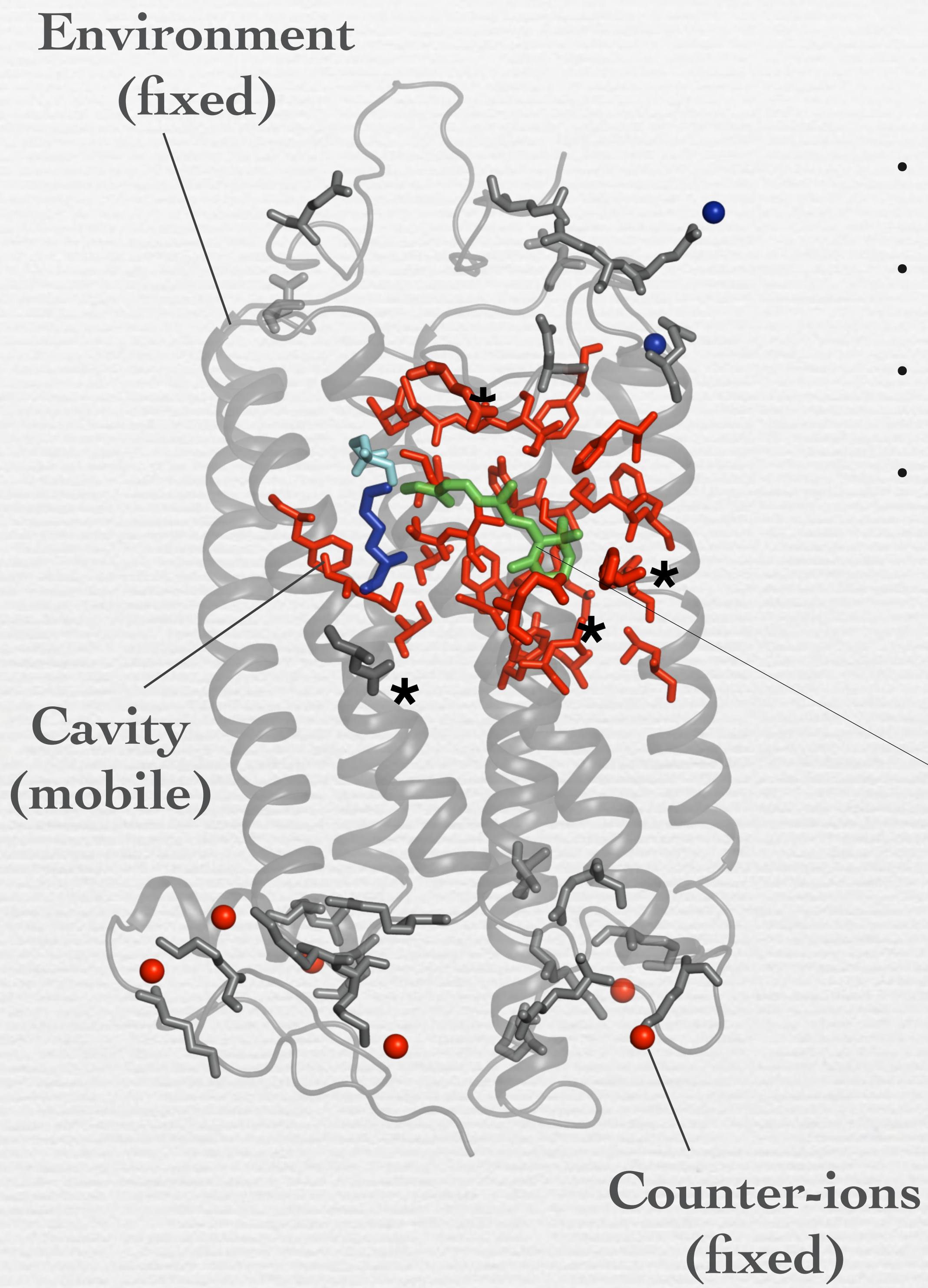

- Gas-phase and globally uncharged monomer
- Chromophore CASPT2//CASSCF/6-31G*
- Electrostatic Embedding, Amber FF (except frontier)
- Only the chromophore, cavity and cavity waters are relaxed

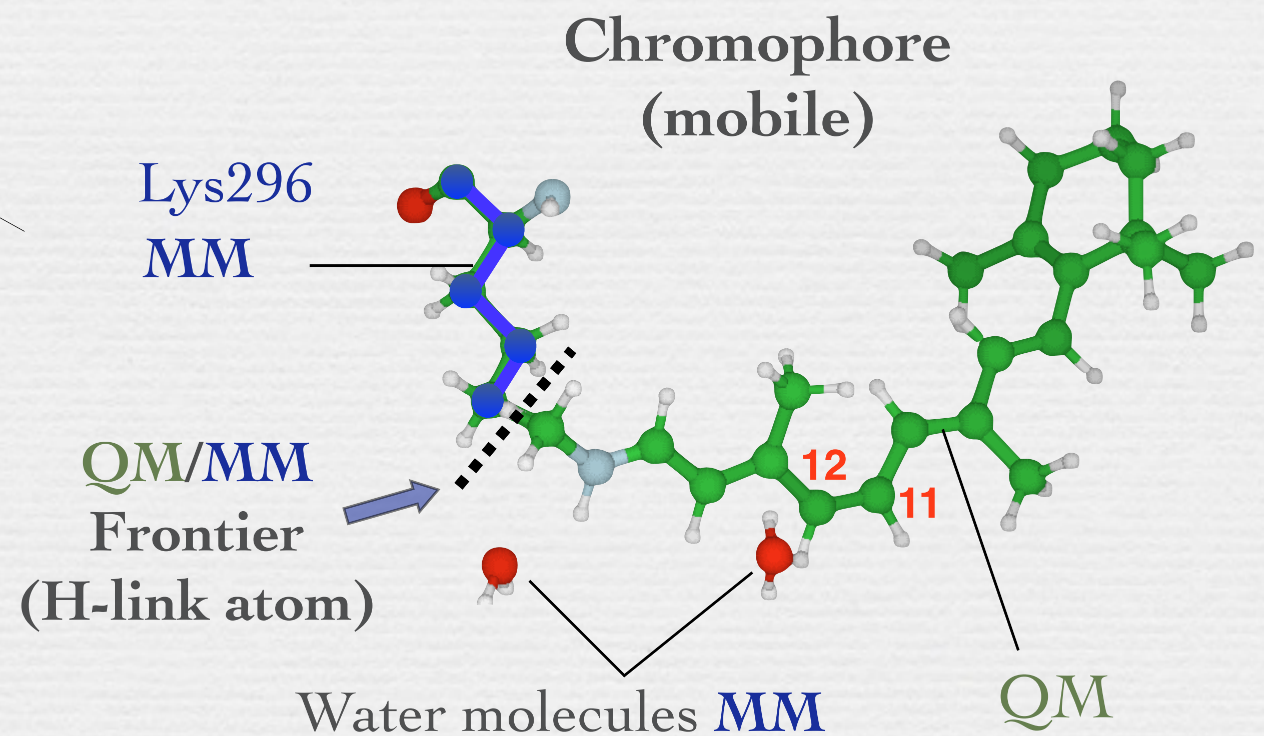

Pedraza-González, L.; De Vico, L.; Marín, M. D. C.; Fanelli, F.; Olivucci, M. *J. Chem. Theory Comput.* **2019**, *15*, 3134-3152.

Automatic rhodopsin modeling (ARM) model benchmark

data from 26 rhodopsins from 18 different organisms (one extinct)

vertebrates, invertebrates, eubacteria and archaea

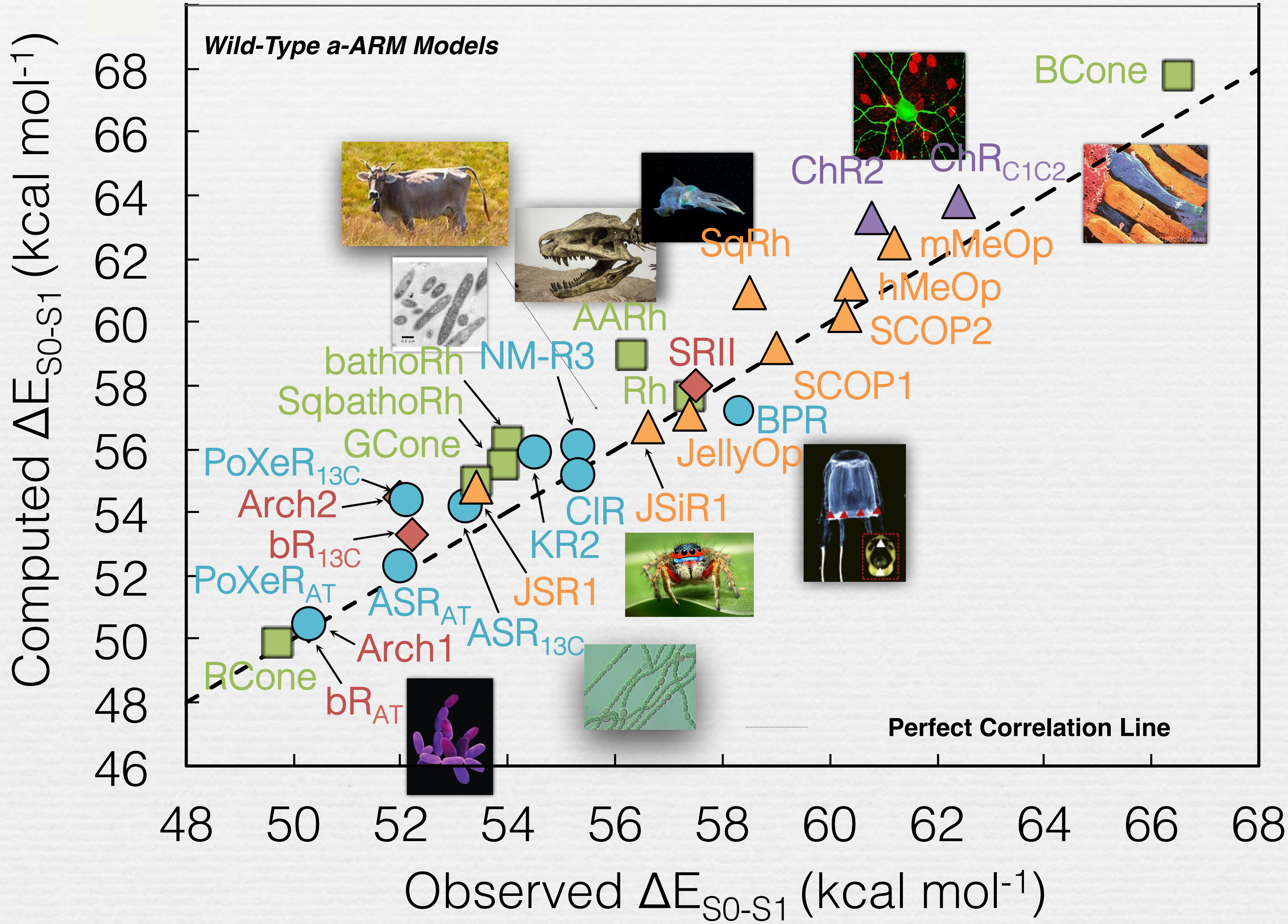

- Pedraza-González, L.; De Vico, L.; Marín, M. D. C.; Fanelli, F.; Olivucci, M. *J. Chem. Theory Comput.* **2019**, *15*, 3134-3152.

(Bovine) Rod Rhodopsin studies using QM/MM models

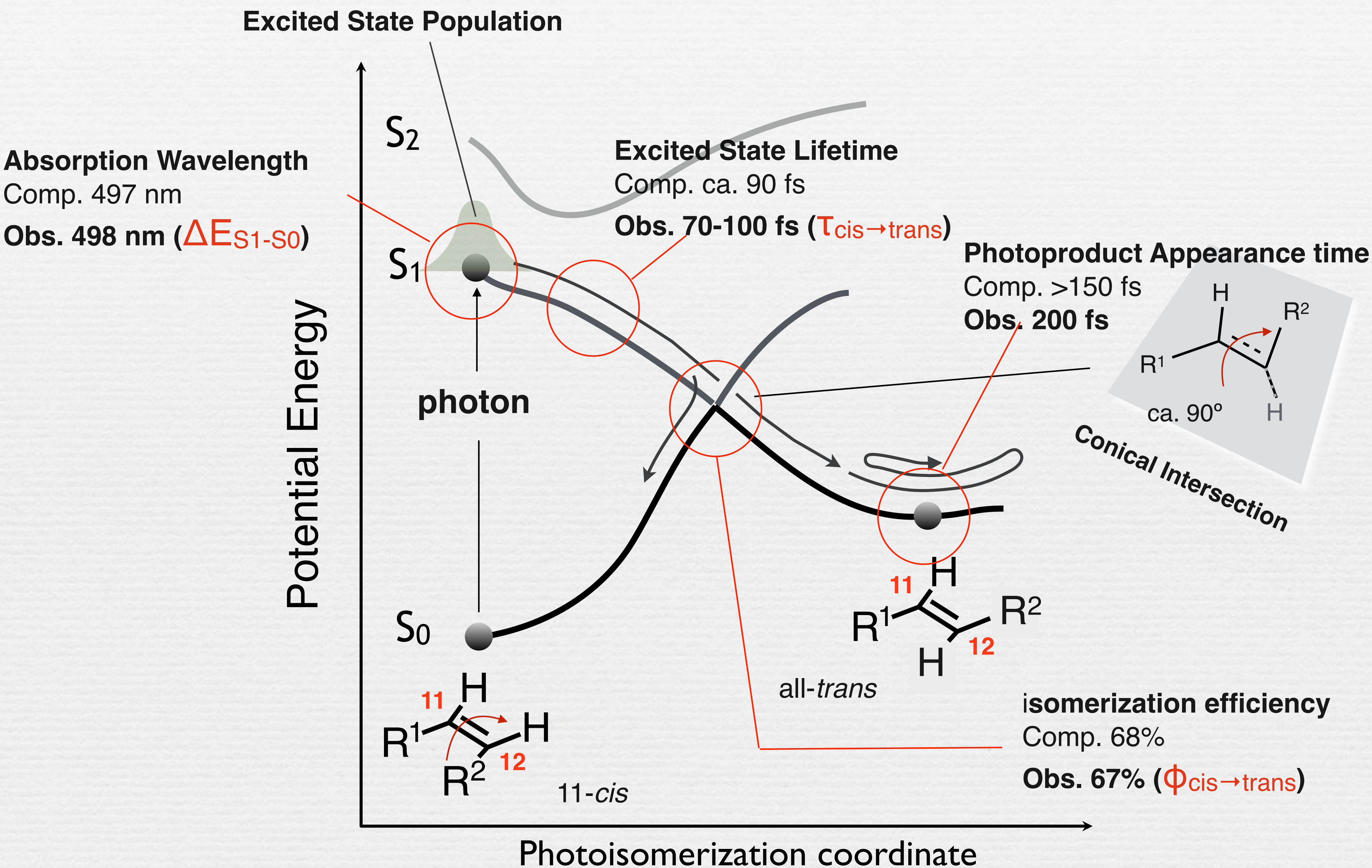

- Gozem, S.; Luk, H. L.; Schapiro, I.; Olivucci, M. *Chem. Rev.* **2017**, *117*, 13502-13565.

Photoisomerization coordinate

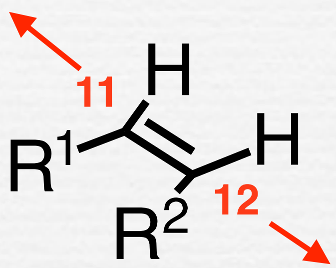

C11=C12 stretching

Comp. ca 22 fs period (~1516 cm^{-1})

Obs. 20 fs, (1679 cm^{-1})

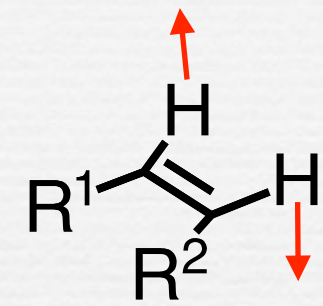

hydrogen out-of-plane (HOOP) wagging

Comp. ca. 40 fs period (~830 cm^{-1})

Obs. 45 fs, (746 cm^{-1})

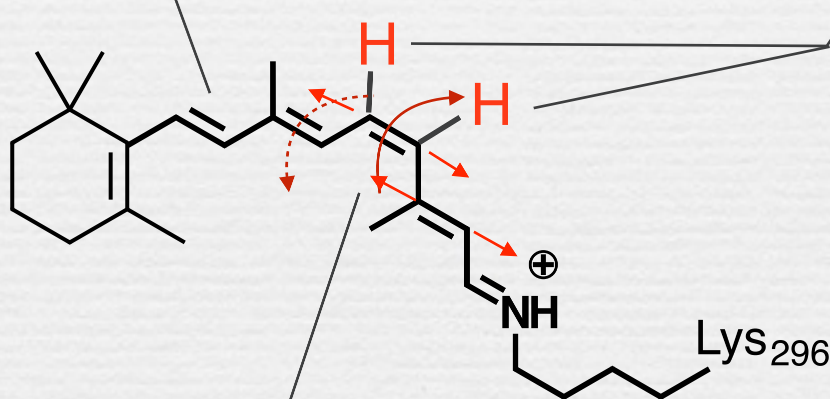

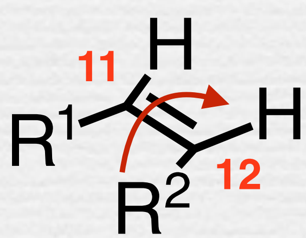

C11=C12 twisting

Comp. 1/4 period ca. 100 fs

Obs. 70-110 fs

- Frutos, L. M.; Andruniów, T.; Santoro, F.; Ferré, N.; Olivucci, M. *Proc. Natl. Acad. Sci. U. S. A.* **2007**, *104*, 7764-7769.
- Polli, D.; Altoè, P.; Weingart, O.; Spillane, K. M.; Manzoni, C.; Brida, D.; Tomasello, G.; Garavelli, M. et al., *Nature* **2010,** *467,* 440.
- Johnson, P. J. M.; Halpin, A.; Morizumi, T.; Prokhorenko, V. I.; Ernst, O. P.; Miller, R. J. D. *Nat. Chem.* **2015***, 7,* 980-6.

Quantum yield calculation using quantum-classical (TSH-GPDC) trajectories

The excited state population dynamics is simulated with **200 QM/MM semi-classical trajectories**

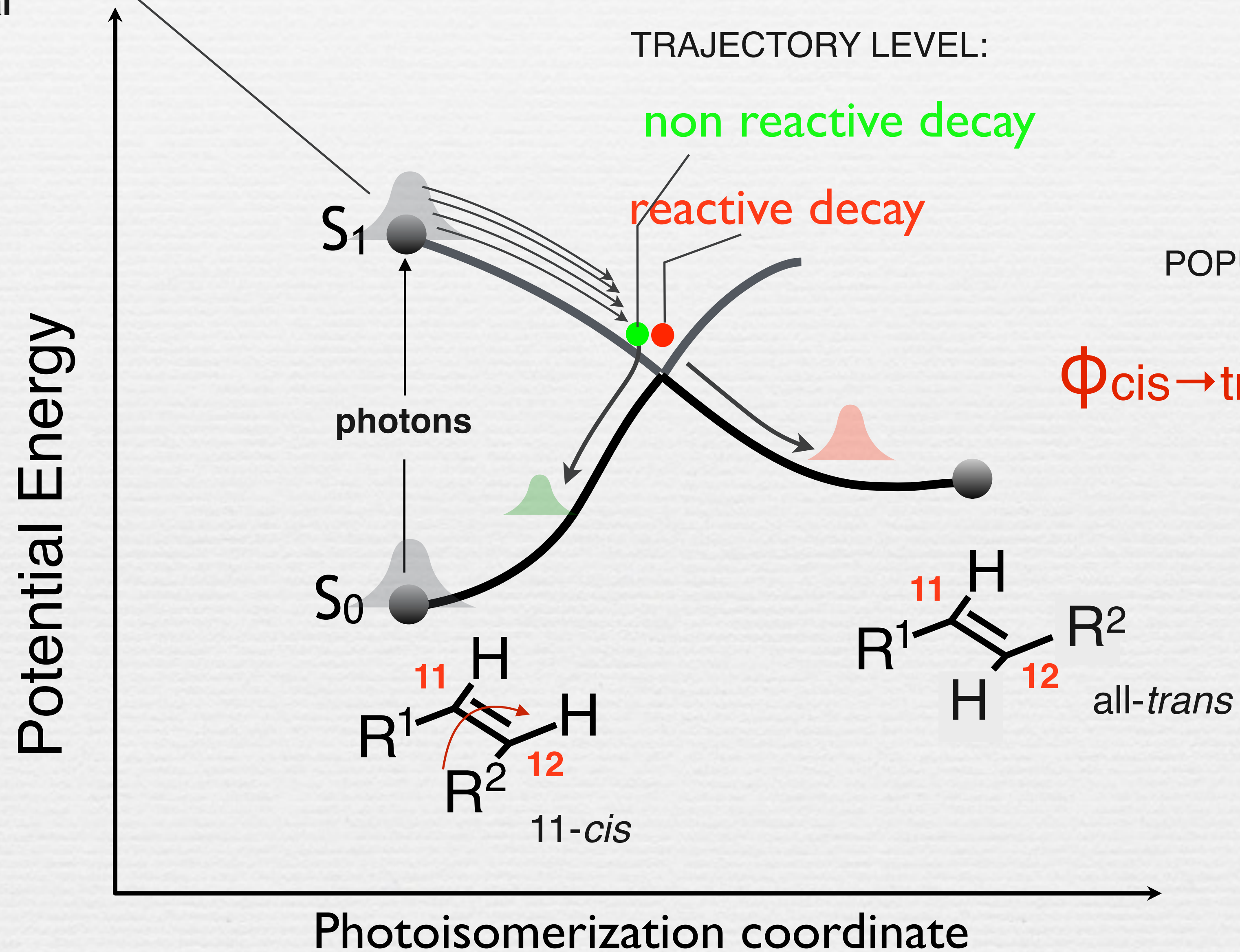

POPULATION LEVEL:

$$\Phi_{cis \rightarrow trans} = \frac{\text{reactive}}{\text{total}}$$

● Gozem, S.; Luk, H. L.; Schapiro, I.; Olivucci, M. *Chem. Rev.* **2017**, *117*, 13502-13565.

Outline

TRAJECTORY LEVEL:

The ***reactivity*** *of each trajectory* is controlled by :

- the **phase and magnitude of the π-overlap velocity** at the decay point

POPULATION (STATISTICAL) LEVEL:

The ***quantum efficiency*** value is controlled by:

- the **splitting (i.d. vibrational decoherence) of the excited state population**

Schnedermann, C.; Yang, X.; Liebel, M.; Spillane, K. M.; Lungtenburg, J.; Fernandez, I.; Valentini, A.; Schapiro, I.; Olivucci, M.; Kukura, P.; Mathies, R. A. *Nat. Chem.* **2018**, *10*, 449-455.

X. Yang; M. Manathunga; S. Gozem; J. Léonard; T. Andruniów; M. Olivucci. *Nat. Chem.* **2022**, *14,* 441-449.

Rhodopsin population dynamics

200 TSH trajectories

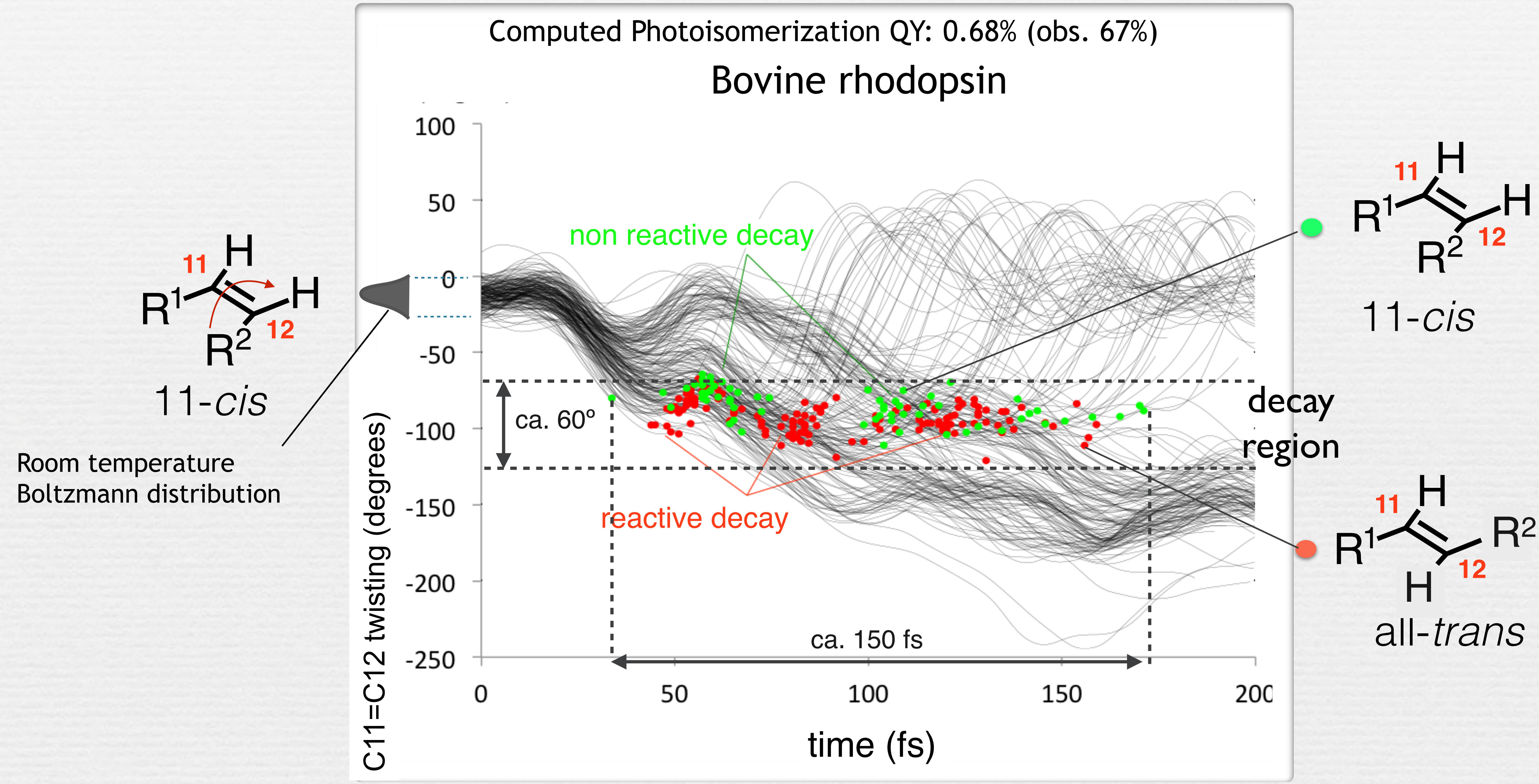

- Schnedermann, C.; Yang, X.; Liebel, M.; Spillane, K. M.; Lungtenburg, J.; Fernandez, I.; Valentini, A.; Schapiro, I.; Olivucci, M.; Kukura, P.; Mathies, R. A. *Nat. Chem.* **2018**, *10*, 449-455.

Rhodopsin population dynamics

200 TSH trajectories

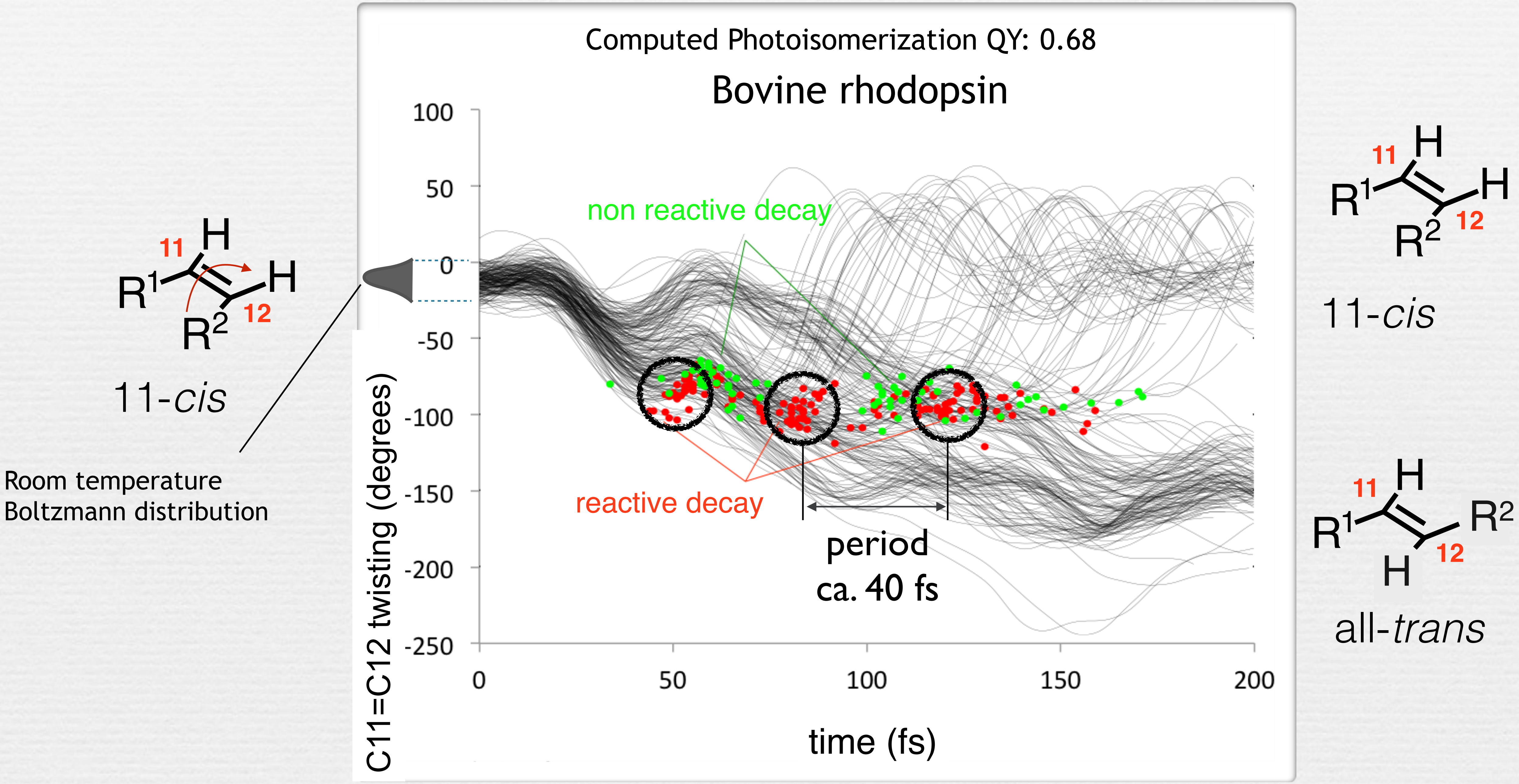

- Schnedermann, C.; Yang, X.; Liebel, M.; Spillane, K. M.; Lungtenburg, J.; Fernandez, I.; Valentini, A.; Schapiro, I.; Olivucci, M.; Kukura, P.; Mathies, R. A. *Nat. Chem.* **2018**, *10*, 449-455.

Rhodopsin population dynamics

200 TSH trajectories

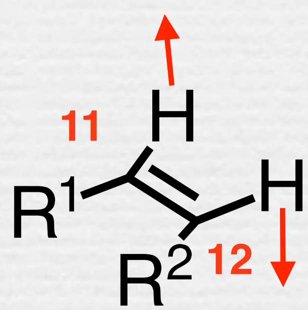

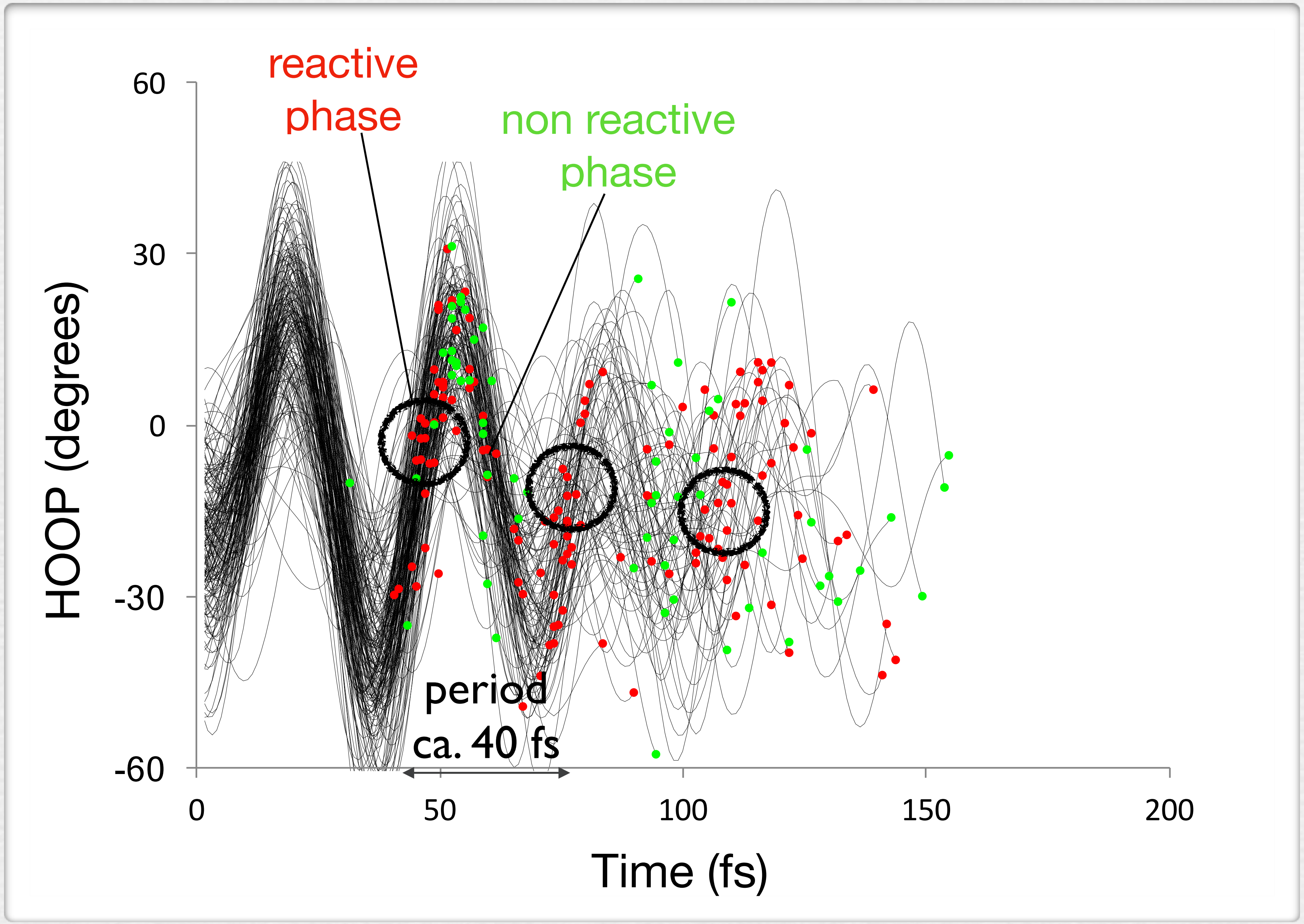

- Schnedermann, C.; Yang, X.; Liebel, M.; Spillane, K. M.; Lungtenburg, J.; Fernandez, I.; Valentini, A.; Schapiro, I.; Olivucci, M.; Kukura, P.; Mathies, R. A. *Nat. Chem.* **2018**, *10*, 449-455.

Relationship between HOOP phase and reactivity

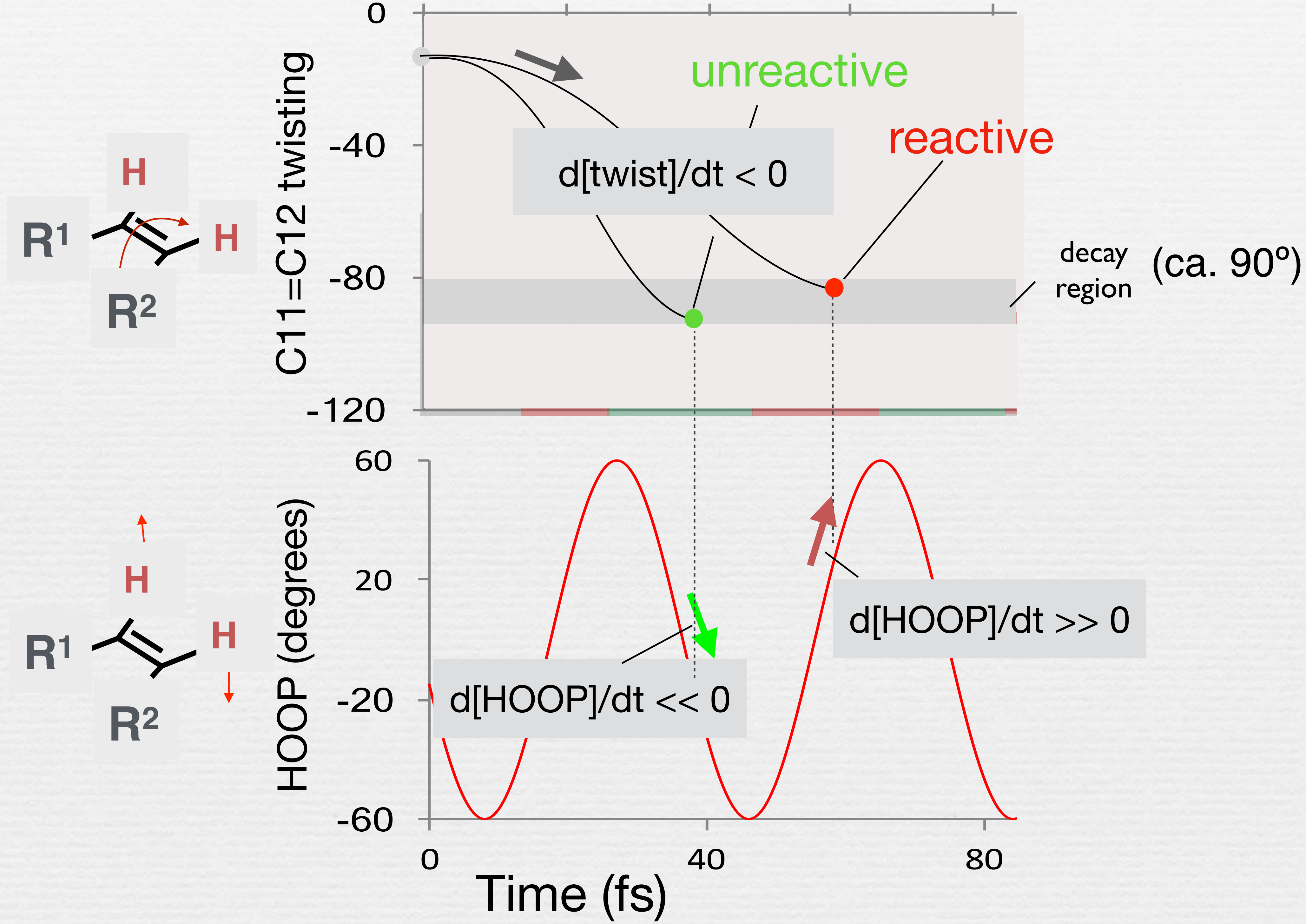

- Klaffki, N.; Weingart, O.; Garavelli, M.; Spohr, E. *Phys. Chem. Chem. Phys.* **2012**, *14*, 14299-14305.
- Schapiro, I.; Ryazantsev, M. N.; Frutos, L. M.; Ferré, N.; Lindh, R.; Olivucci, M. *J. Am. Chem. Soc.* **2011**, *133*, 3354-3364.

Relationship between overlap velocity and reactivity

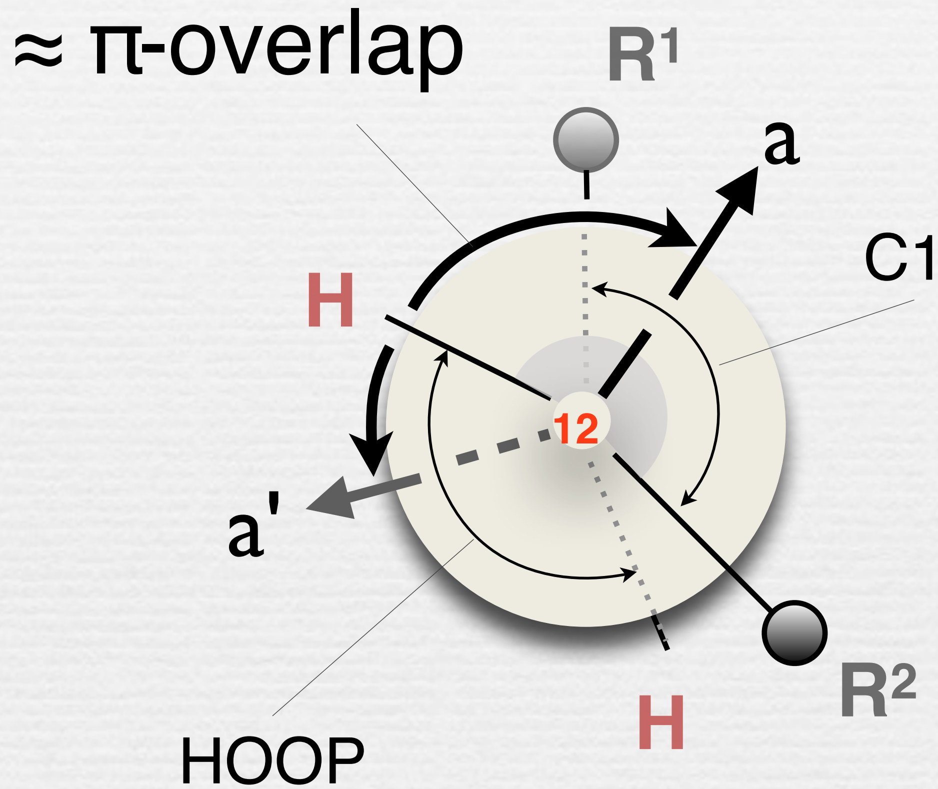

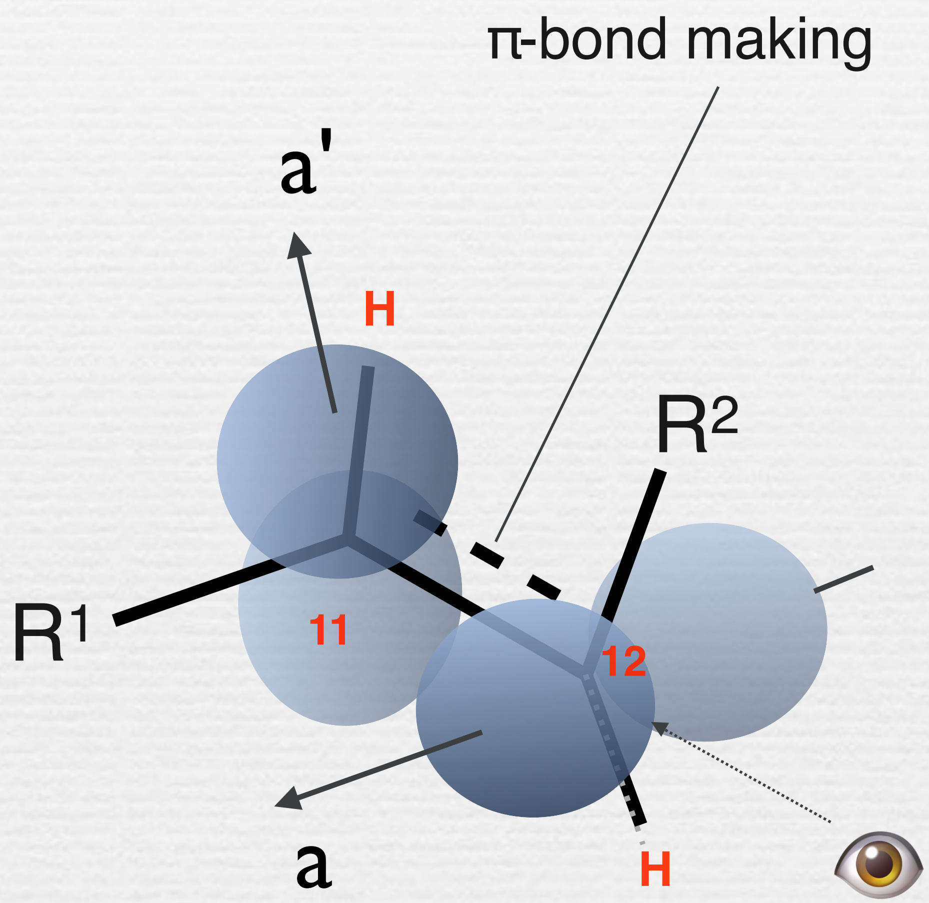

$$\approx \pi\text{-overlap} = (\text{Twist-HOOP})/2$$

Relationship between overlap velocity and reactivity

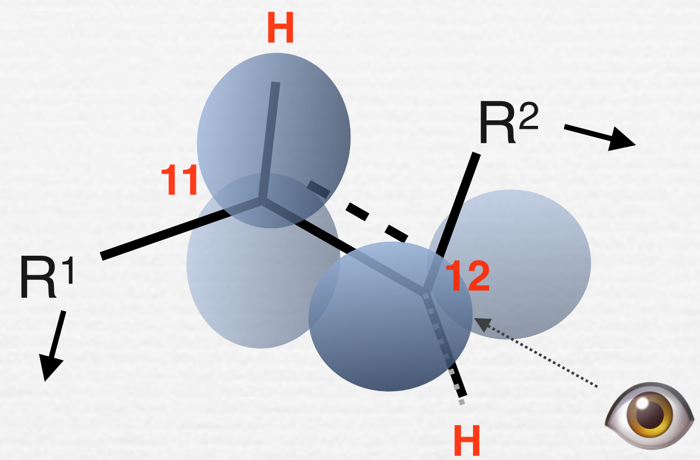

the orbital overlap is ca. zero at decay

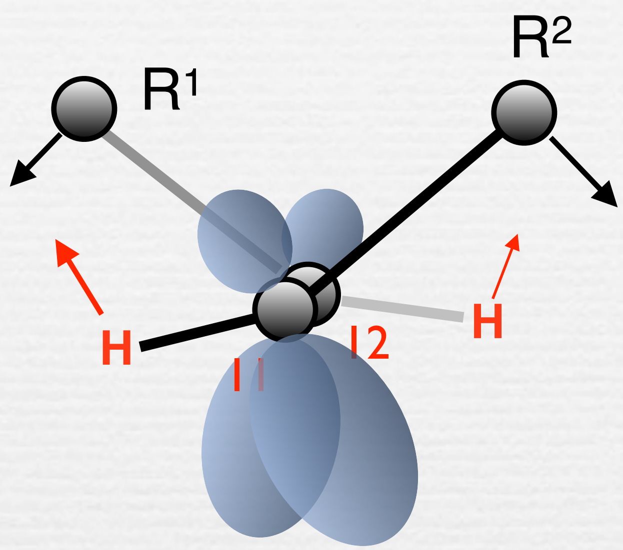

Increasing HOOP

d[overlap]/dt < 0

to all-*trans*

(reactive)

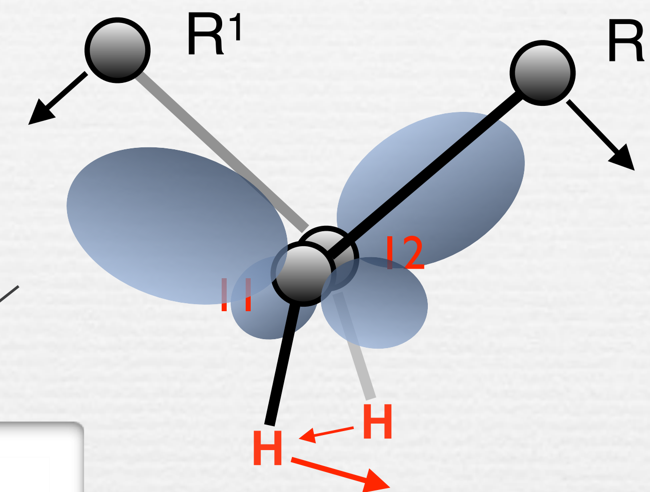

Decreasing HOOP

d[overlap]/dt > 0

to 11-*cis*

(unreactive)

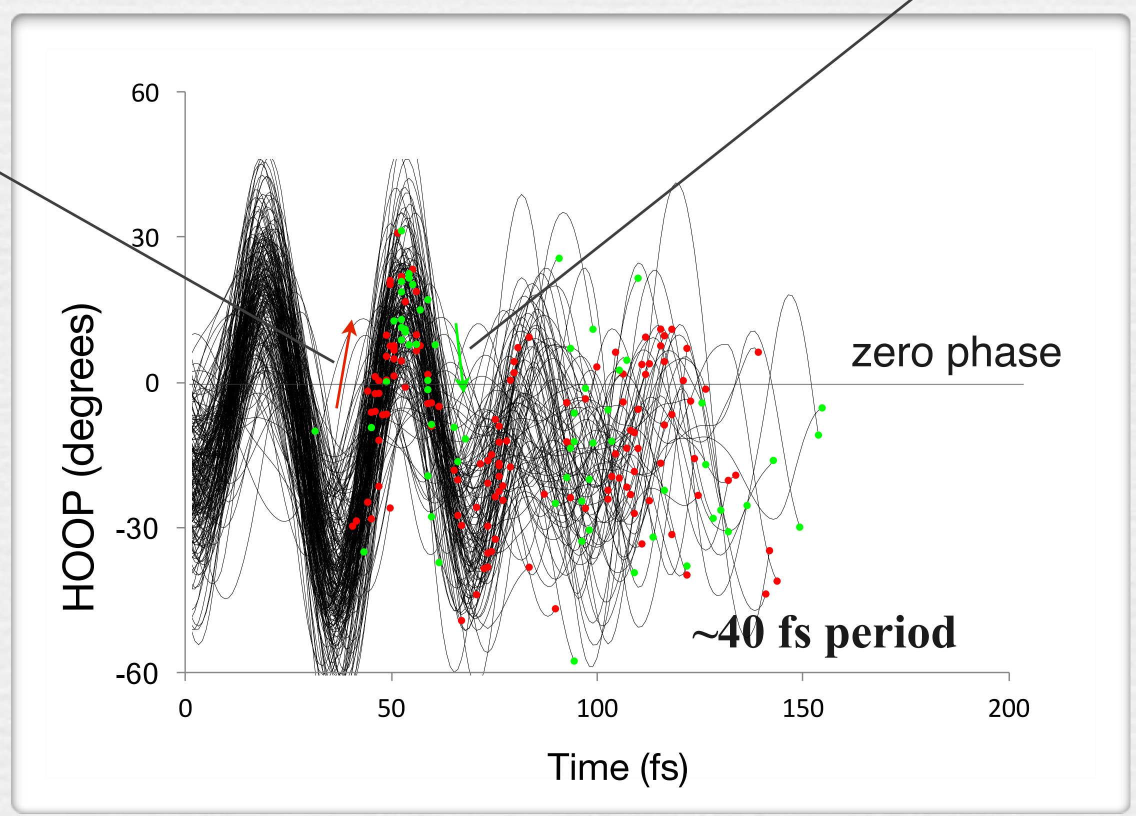

- Weingart, O. *Chem. Phys.* **2008**, *349*, 348-355.
- Klaffki, N.; Weingart, O.; Garavelli, M.; Spohr, E. *Phys. Chem. Chem. Phys.* **2012**, *14*, 14299-14305.
- Schapiro, I.; Ryazantsev, M. N.; Frutos, L. M.; Ferré, N.; Lindh, R.; and Olivucci, M. *J Am Chem Soc* **2011**, *133*, 3354–3364.

Relationship between overlap velocity and quantum efficiency

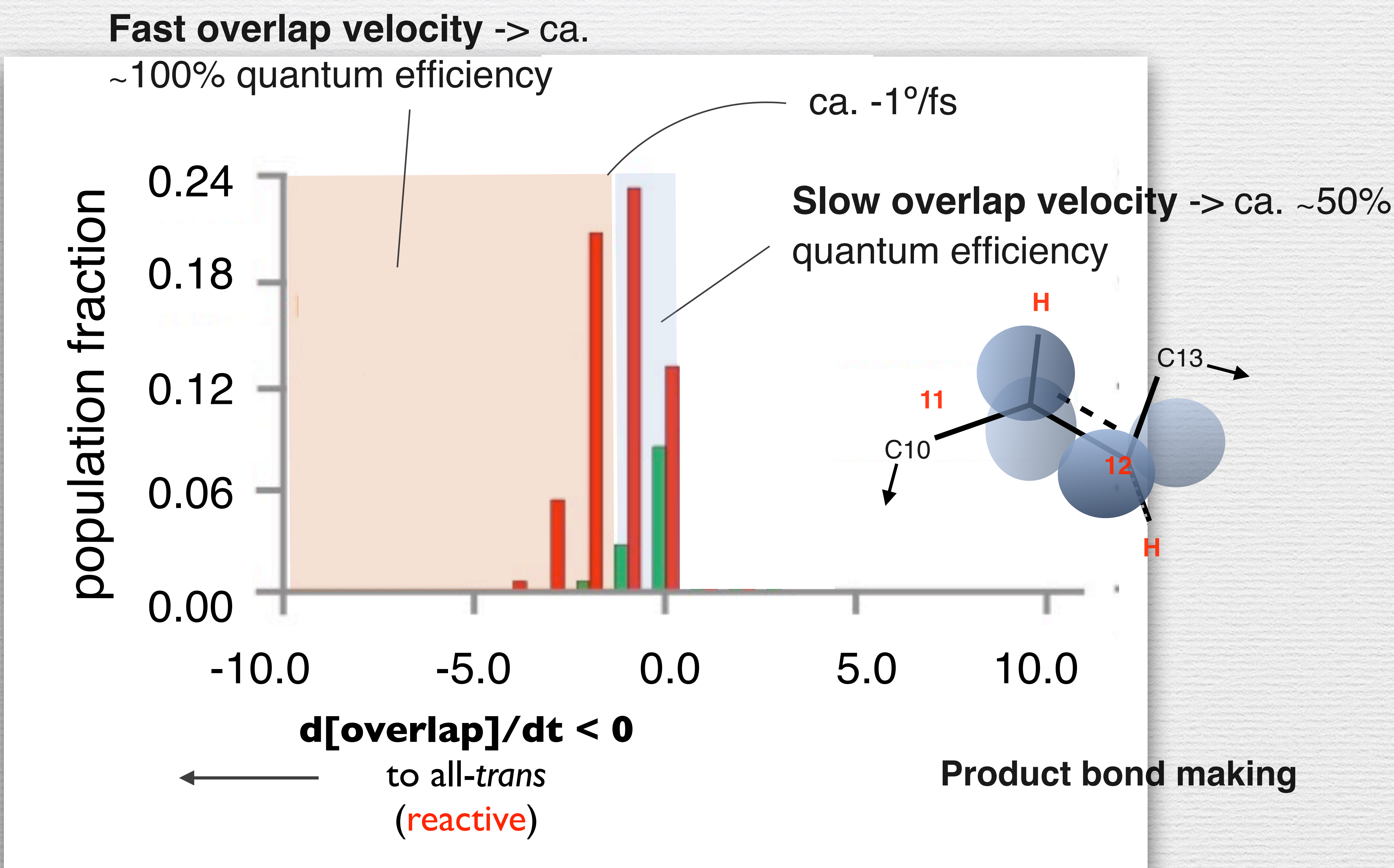

- Gonzalez Blanco, A., Olivucci, M. et al. in preparation

Population dynamics and quantum efficiency

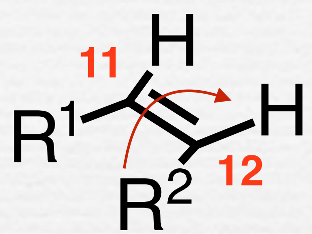

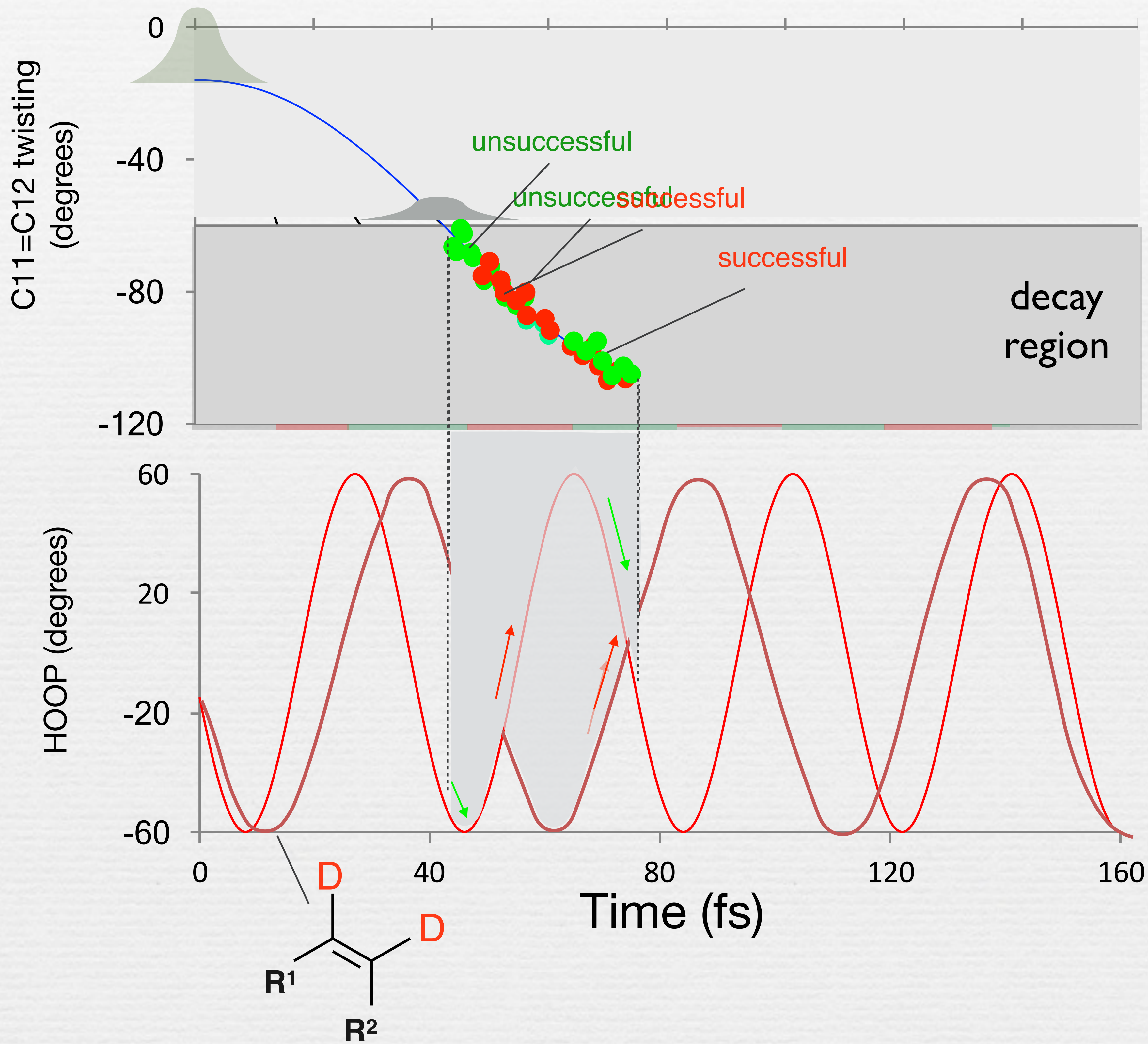

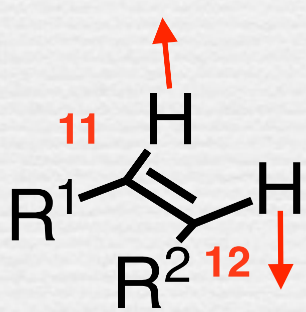

- Schnedermann, C.; Yang, X.; Liebel, M.; Spillane, K. M.; Lungtenburg, J.; Fernandez, I.; Valentini, A.; Schapiro, I.; Olivucci, M.; Kukura, P.; Mathies, R. A. *Nat. Chem.* **2018**, *10*, 449-455.

The phase relationship between HOOP and twisting determines the reactivity

Coworkers: R. A. Mathies, P. Kukura, J.Lugtenburg

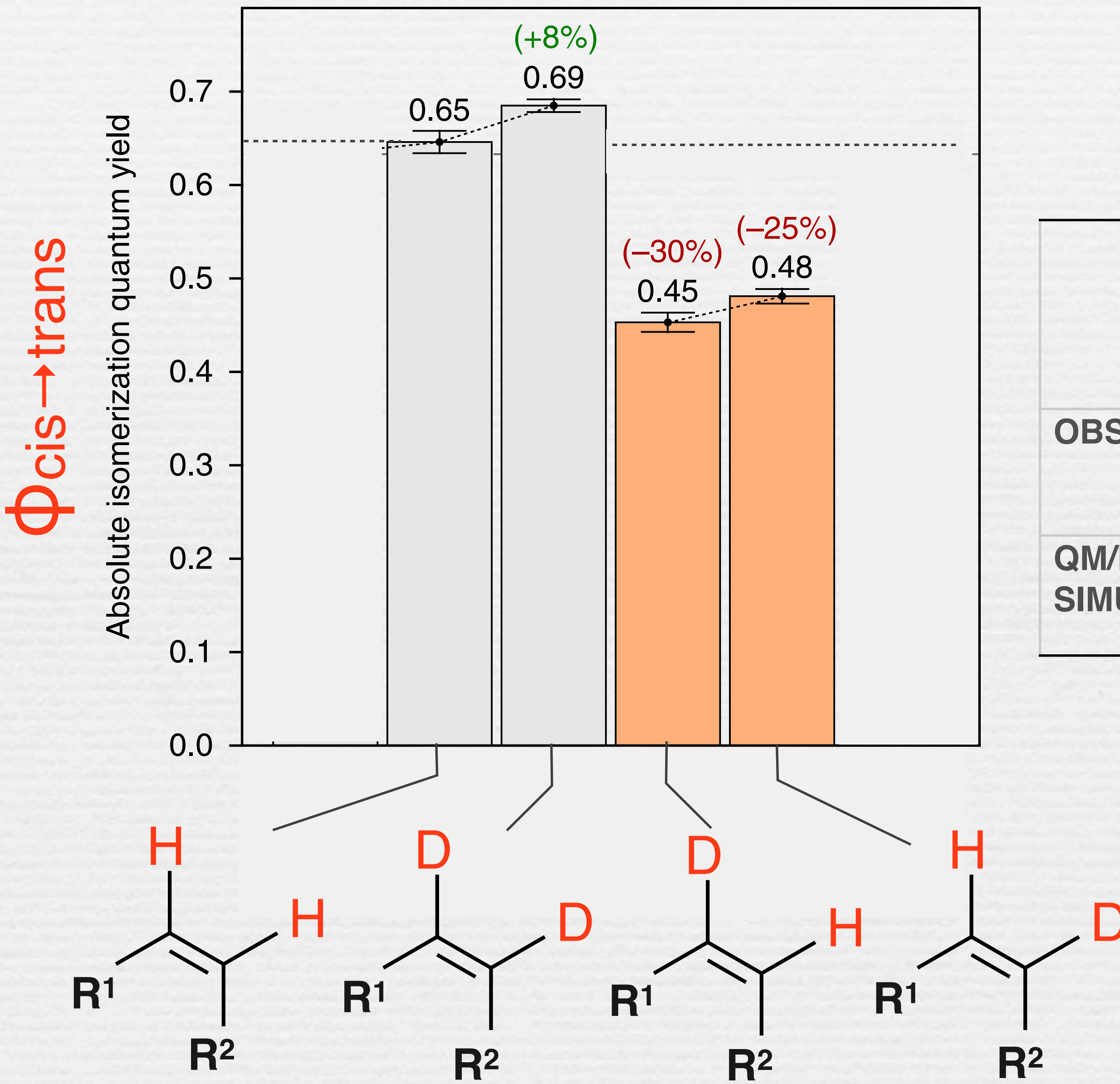

	Quantum yield WT	Quantum yield 11D	
OBSERVED	**0.65**	0.45 (-30%)	
QM/MM SIMULATED	**0.68**	0.62 (-14%)	

- Schnedermann, C.; Yang, X.; Liebel, M.; Spillane, K. M.; Lungtenburg, J.; Fernandez, I.; Valentini, A.; Schapiro, I.; Olivucci, M.; Kukura, P.; Mathies, R. A. *Nat. Chem.* **2018**, *10*, 449-455.

CT-MQC Quantum-Classical Trajectories for a Model Chromophore:

Coworkers: E. Marsili, F. Agostini, D. Lauvergnat

Couple-Trajectory mixed Quantum-Classical (based on exact factorization)

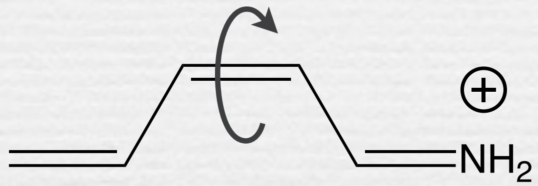

(Parametrized 3D PES)

Tully SH with Energy Decoherence Correction

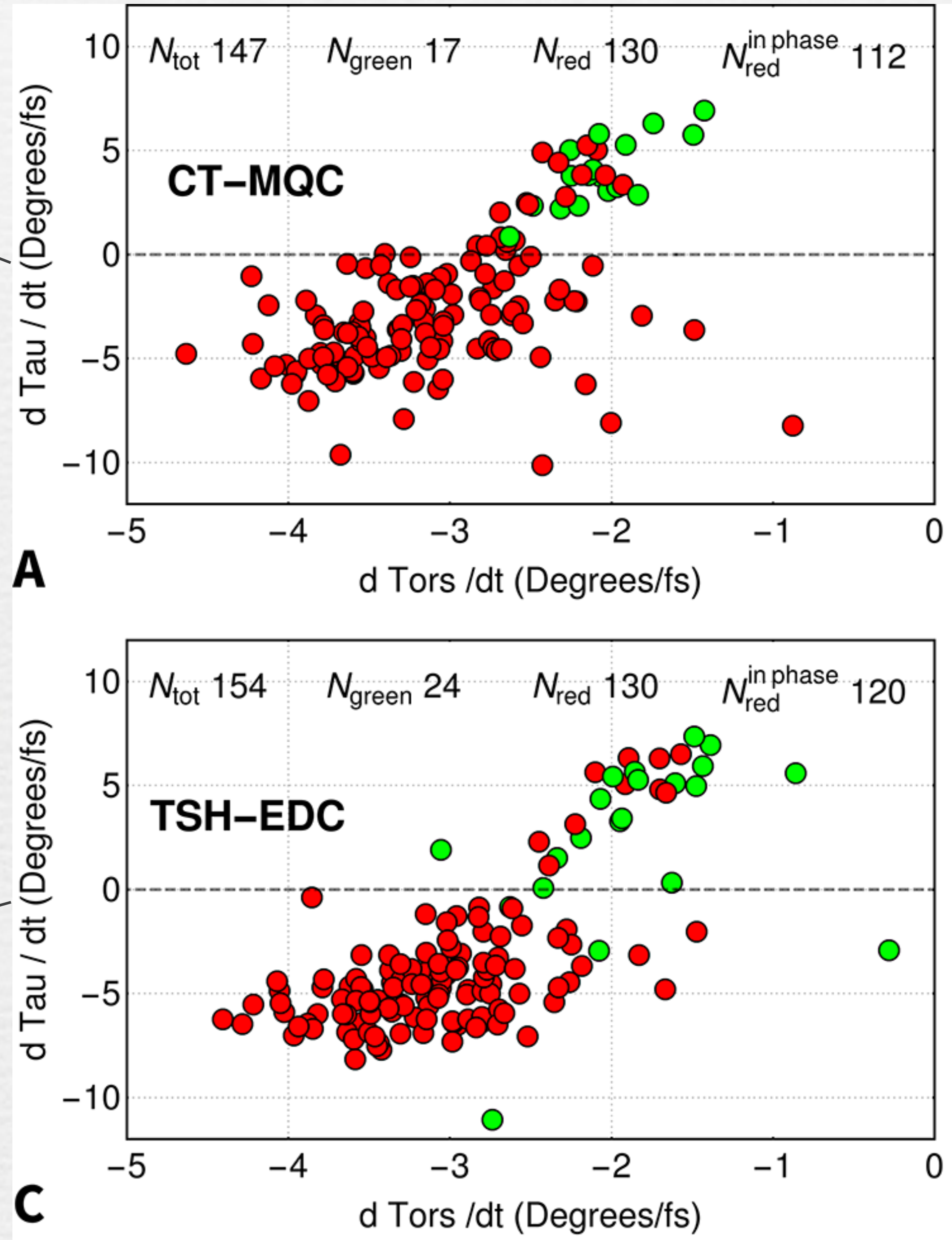

- E. Marsili; M. H. Farag; Y. Xuchun; L. De Vico; M. Olivucci. *J. Phys. Chem. A* 2019, **123**, 1710-1719.
- E. Marsili; M. Olivucci; D. Lauvergnat; F. Agostini. *J. Phys. Chem. A* 2020, **16**, 6032-6048.

Rhodopsin population dynamics

200 TSH trajectories

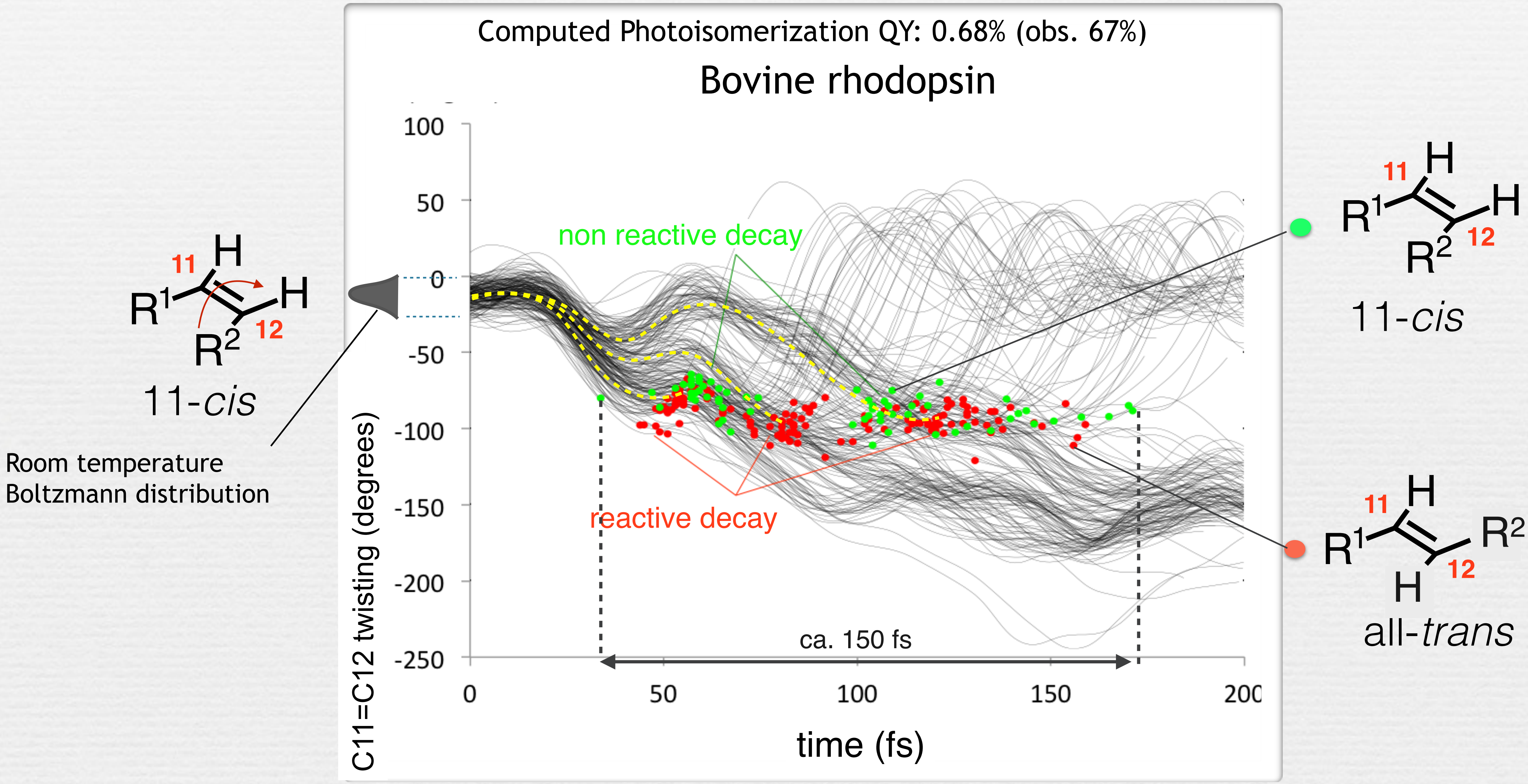

- X. Yang; M. Manathunga; S. Gozem; J. Léonard; T. Andruniów; M. Olivucci. *Nat. Chem.* 2022, **14**, 441-449.

Fast and slow population dynamics

200 TSH trajectories

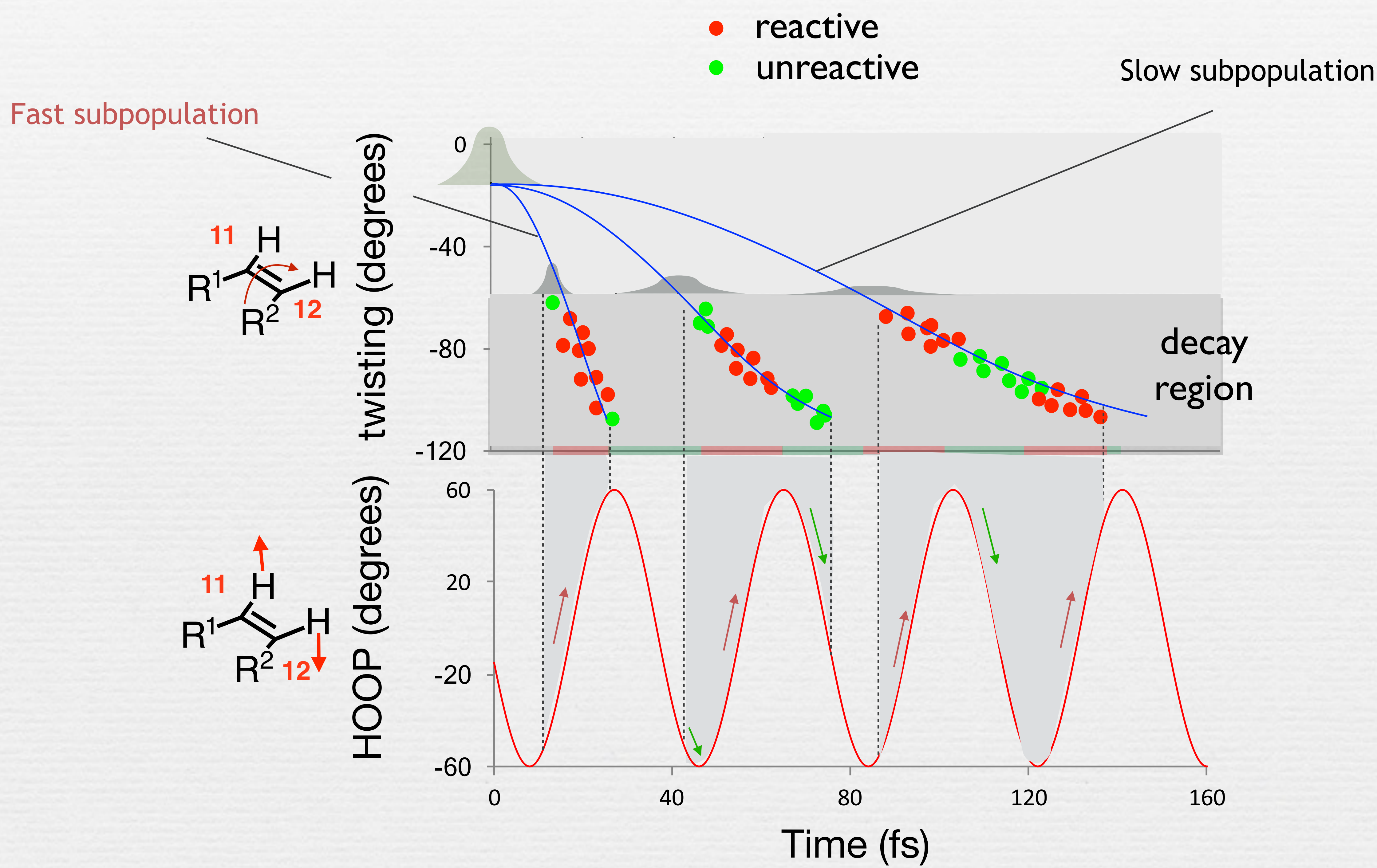

- X. Yang; M. Manathunga; S. Gozem; J. Léonard; T. Andruniów; M. Olivucci. *Nat. Chem.* 2022, **14**, 441-449.

Fast and slow subpopulation dynamics

50 fast + 50 slow TSH trajectories

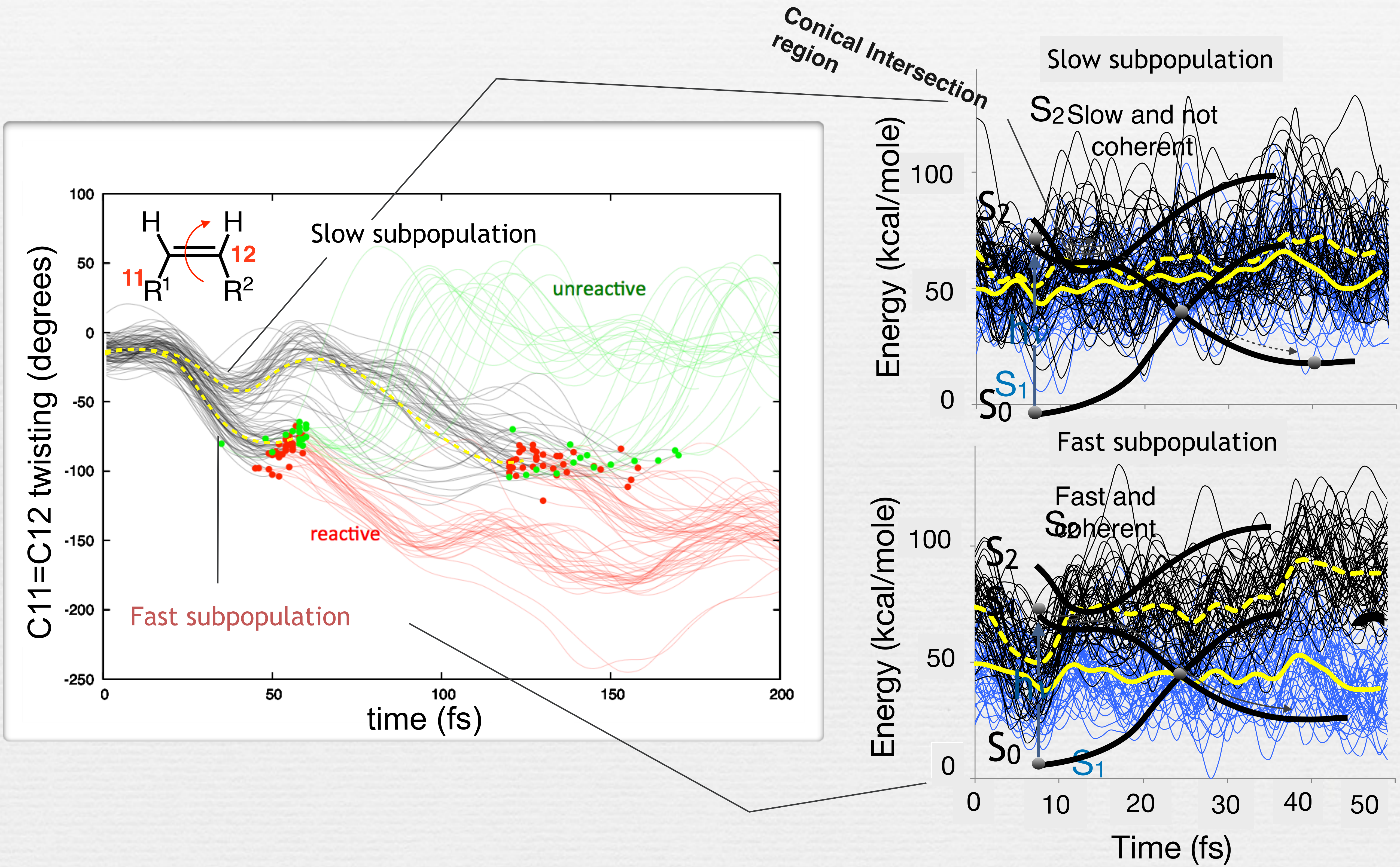

- X. Yang; M. Manathunga; S. Gozem; J. Léonard; T. Andruniów; M. Olivucci. *Nat. Chem.* 2022, **14**, 441-449.

Resonance Raman spectra simulations

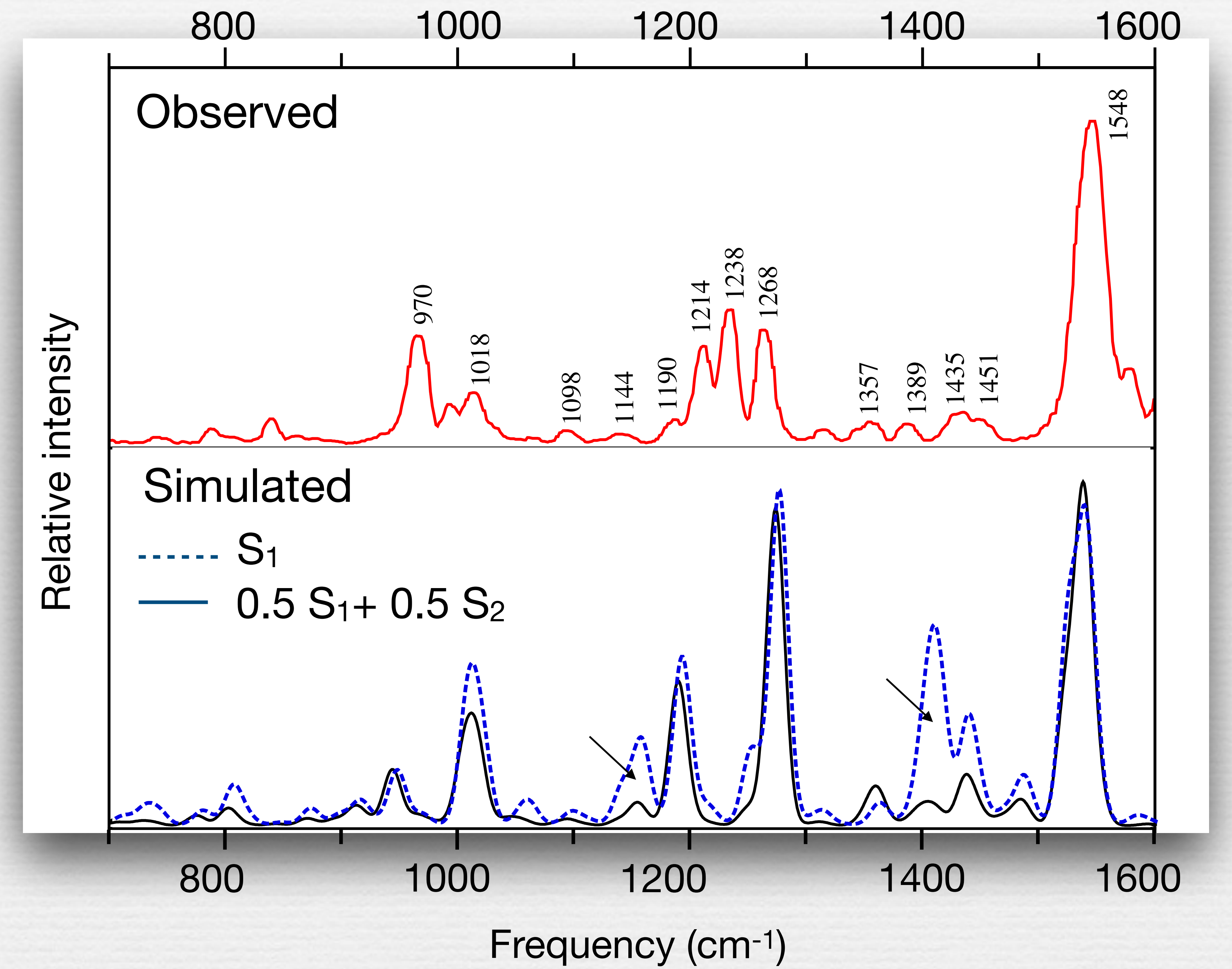

- X. Yang; M. Manathunga; S. Gozem; J. Léonard; T. Andruniów; M. Olivucci. *Nat. Chem.* 2022, **14**, 441-449.

20 fs Gaussian Wavepacket Dynamics for a Model Chromophore

Coworkers: M. A. Robb, G. A. Worth

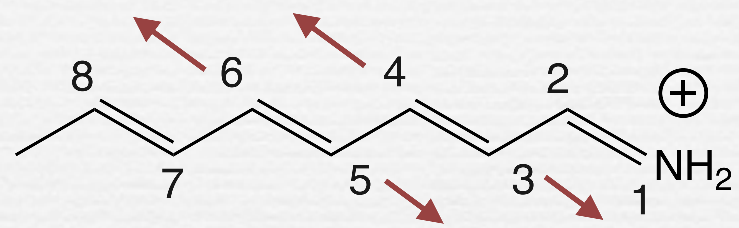

Initial electronic
No-mixing

Initial S_2/S_1 electronic
mixing

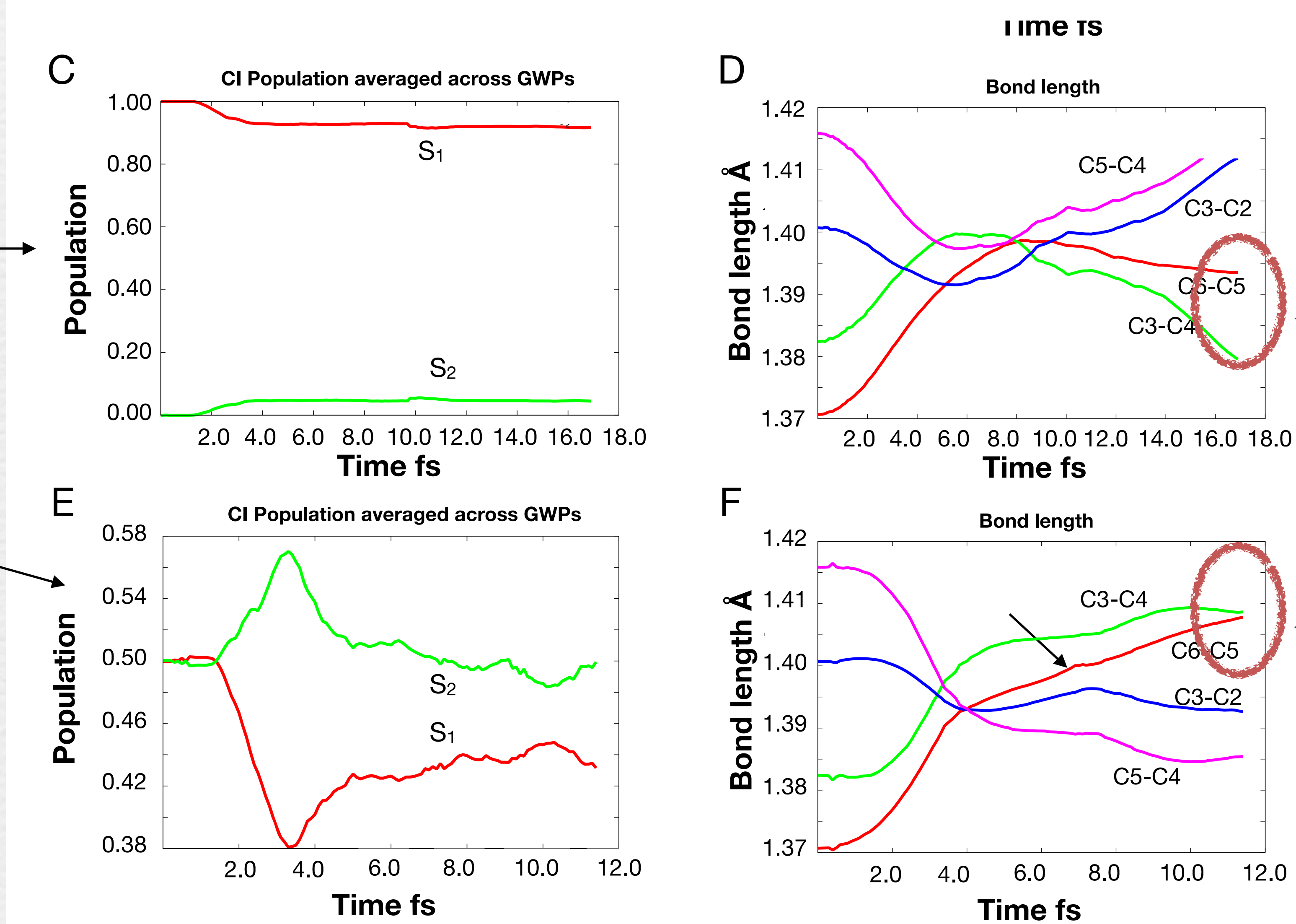

1.39 Å

ca. 1.41 Å

- M. Olivucci; T. Tran; G. A. Worth; M. A. Robb. *J. Phys. Chem. Lett.* **2021**, *12*, 5639-5643.

May biological evolution have tuned the population splitting ?

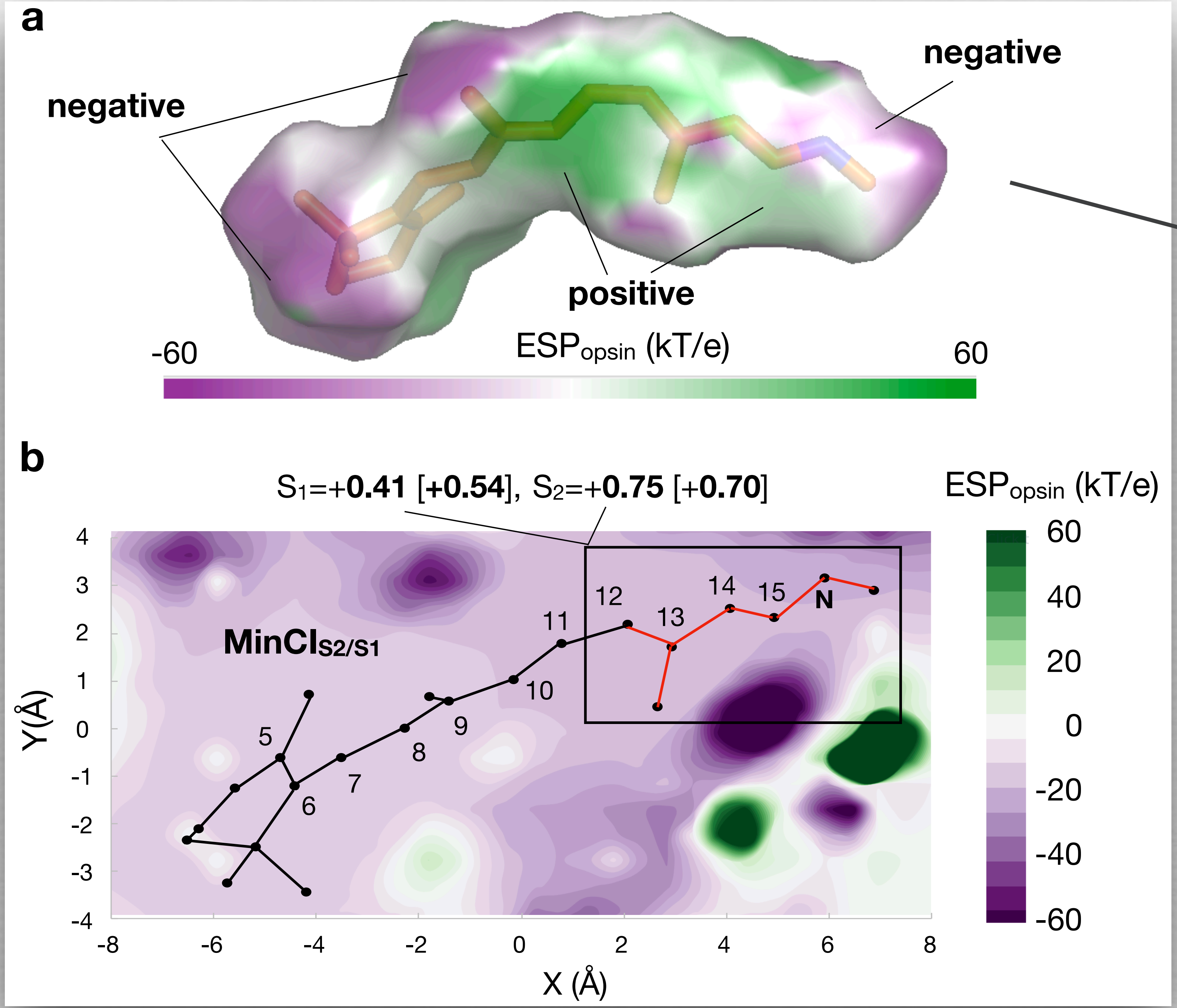

ELECTROSTATIC FIELD PROJECTED BY THE PROTEIN CAVITY ON THE CHROMOPHORE SURFACE

- Yang, X.; Manathunga, M.; Gozem, S.; Léonard, J.; Andruniów, T.; Olivucci, M. Nat. Chem. in press.

May biological evolution have tuned the population splitting ?

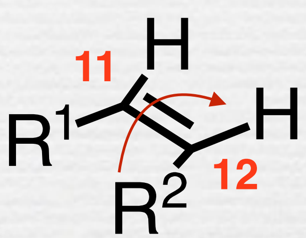

Original protein charges | Halved protein charges

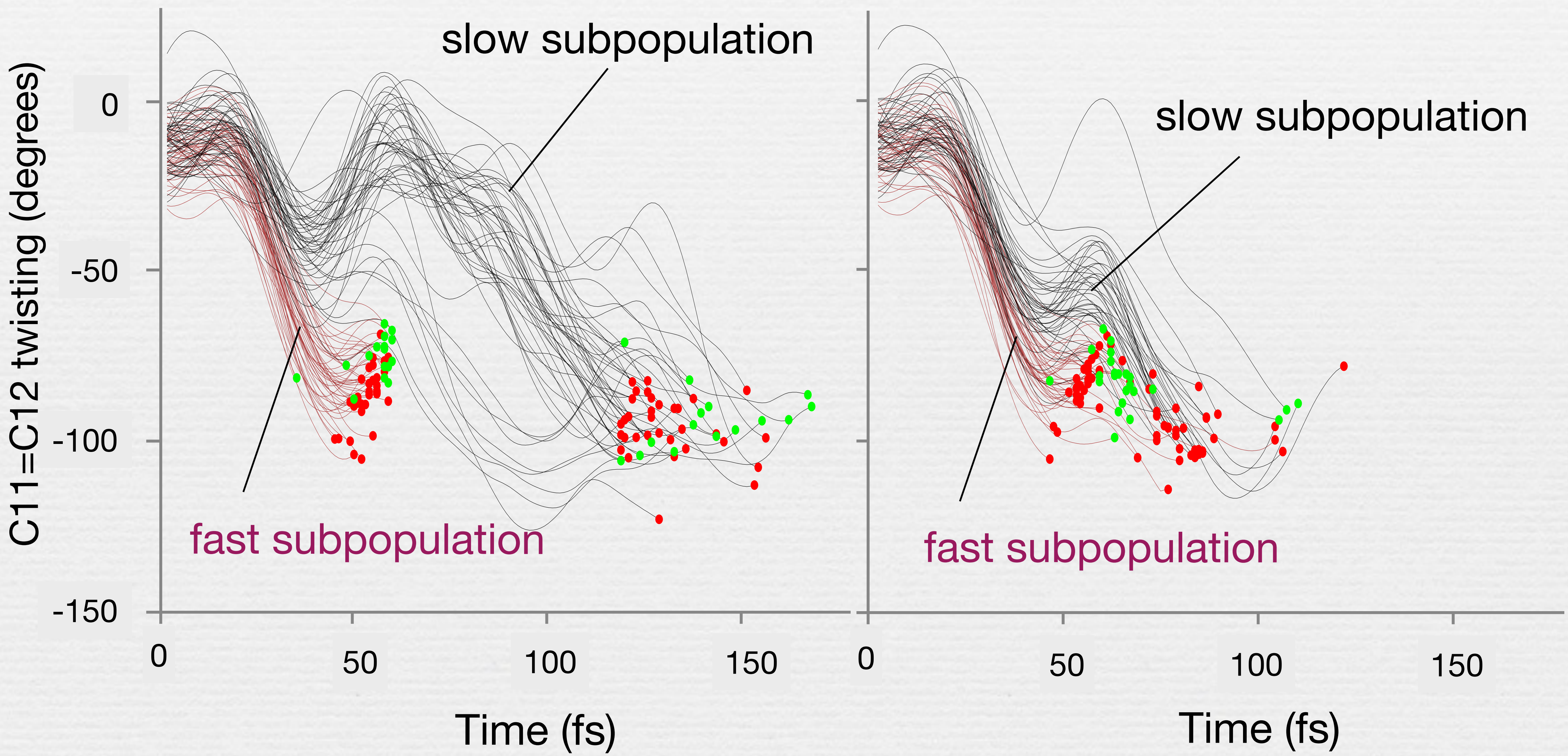

Isomerization quantum yield 68% | Isomerization quantum yield 72%

- Yang, X.; Manathunga, M.; Gozem, S.; Léonard, J.; Andruniów, T.; Olivucci, M. Nat. Chem. in press.

Jumping Spider rhodopsin population dynamics

(with X. Yang)

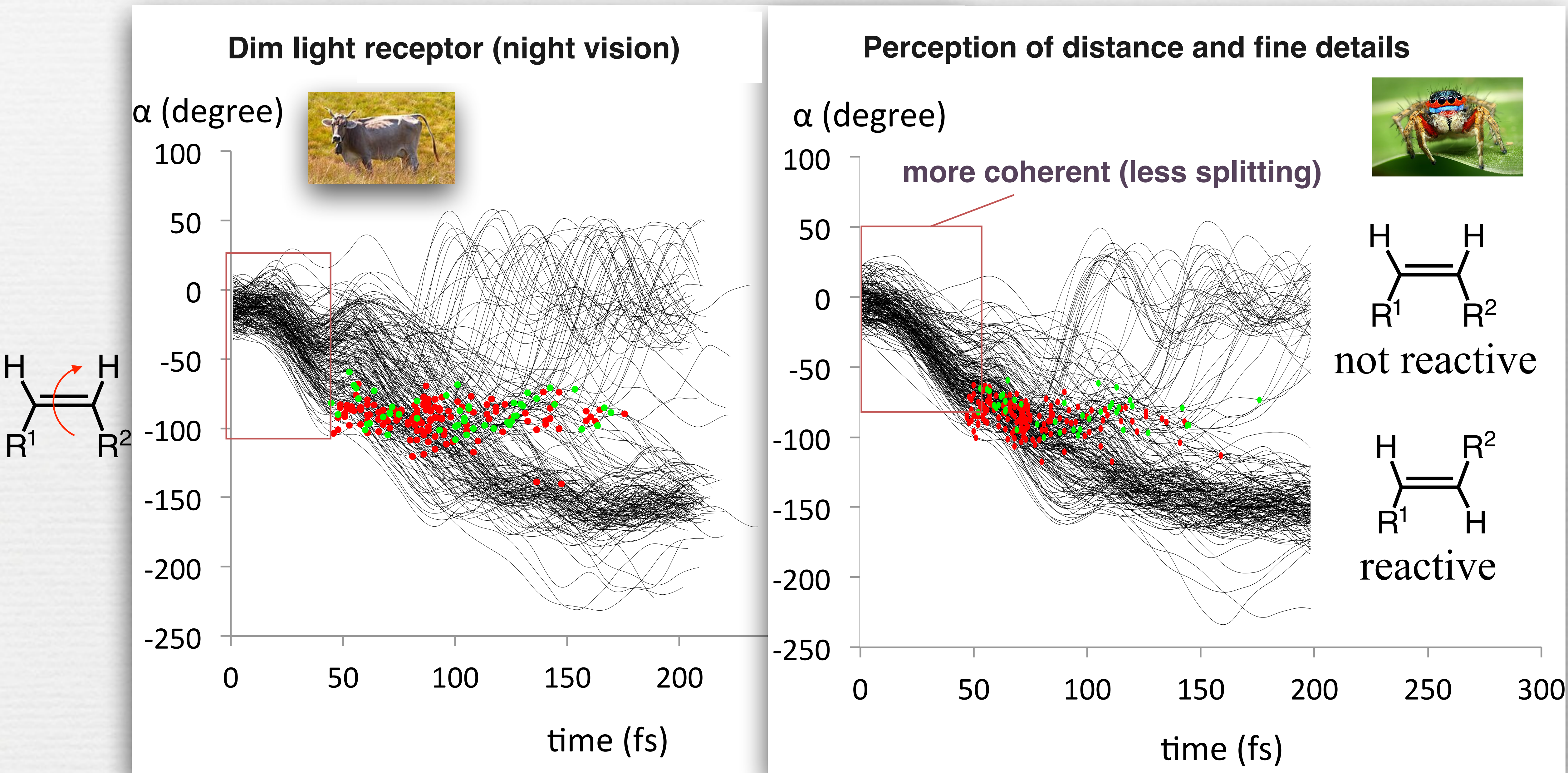

Absorption Max ca. 497 nm (Obs. 498)
Excited State Lifetime ca. 100 fs (Obs. 70 to100)
Isomerization Quantum Yields ca. 72% (Obs. 67%)

Absorption Max ca. 542 nm (Obs. 535)
Excited State Lifetime 83 fs
Isomerization Quantum Yields 78%

Conclusion & Perspectives

The quantum efficiency ($\phi_{cis \rightarrow trans}$) of rod rhodopsins is controlled by **two conical intersections**:

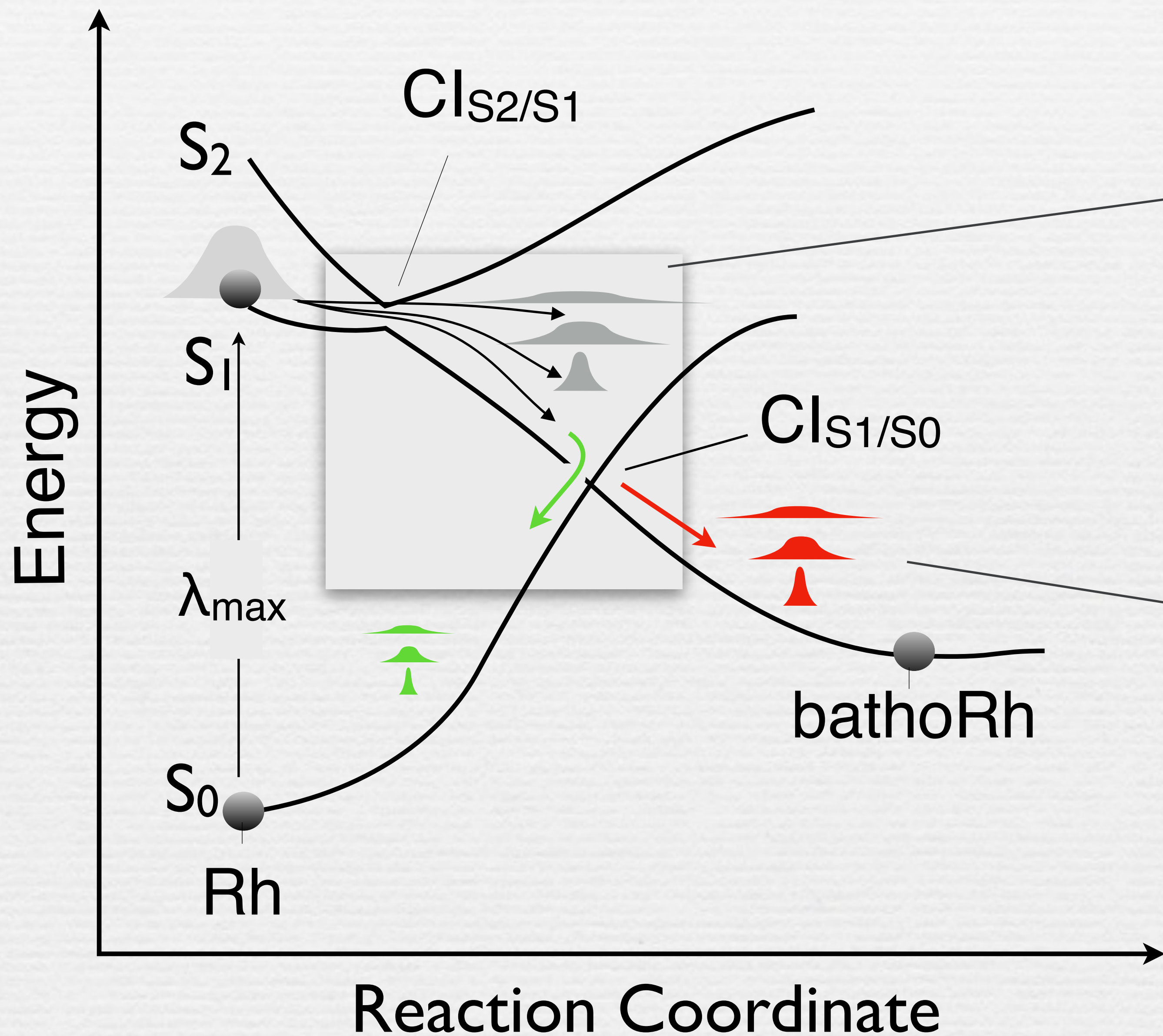

S2/S1 mixing

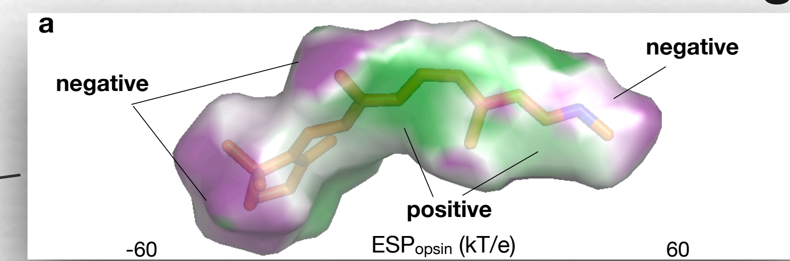

splitting of the S1 population in subpopulations

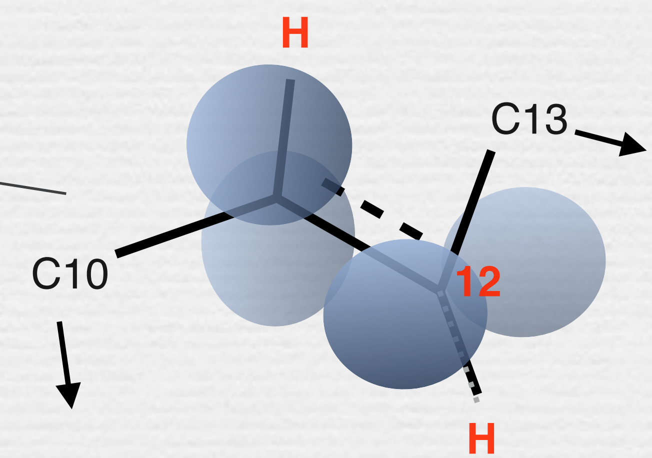

total fraction of the S1 population with **d[overlap]/dt < 0**

Yang, X.; Manathunga, M.; Gozem, S.; Léonard, J.; Andruniów, T.; Olivucci, M. Nat. Chem. in press.